Graphene and its unique properties

A. Castro-Neto (Boston U.), N. M. R. Peres (U. Minho, Portugal), E. V. Castro, J. dos Santos (Porto), J. Nilsson (Boston, U, Göteborg.), A. Morpurgo (Delft), M. I. Katsnelson (Nijmegen), D. Huertas-Hernando (Trondheim, Norway), D. P. Arovas, M. M. Fogler (U. C. San Diego), J. González, F. G., G. León, M. P. López-Sancho, T. Stauber, J. A. Vergés, M. A. H. Vozmediano, B Wunsch (CSIC, Madrid), A. K. Geim, K. S. Novoselov (U. Manchester), A. Lanzara (U. C. Berkeley), M. Hentschel (Dresden), E. Prada, P. San-José (Karlsruhe, Lancaster), J. L. Mañes (U. País Vasco, Spain), F. Sols (U. Complutense, Madrid), E. Louis (U. Alicante, Spain), A. L. Vázquez de Parga, R. Miranda, M. M. Ugeda, I. Brihuega, J. M. Gómez-Rodríguez (U. Autónoma, Madrid), B. Horovitz (Beersheva), P. Le Doussal (ENS, Paris), A. K. Savchenko (Exeter), F. von Oppen (Berlin), A. Akhmerov (Leyden), M. Wimmer (Regensburg, Leyden), T. Low (Purdue), V. Parente, A. Tagliacozzo (Naples), D. Rainis, F. Taddei, M. Polini (Pisa), V. I. Fal'ko (Lancaster), M. F. Crommie (UC Berkeley), H. Manoharan (Stanford)

2nd Workshop on Nanoscience: Carbon-Related Systems and Nanomaterials
Tainan, Taiwan, July 2012

Outline

- Basic facts about graphene
- Graphene as a membrane: gauge fields
- Electron-electron interactions in graphene

Related materials

Graphite intercalation compounds:

Doped graphene planes.

Superconducting at low temperatures.

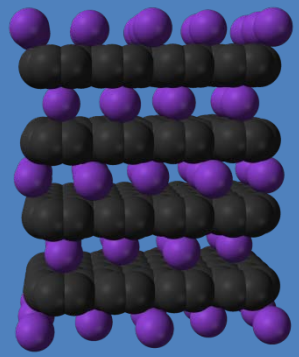

Polyacetylene:

π-bonded chain.

Peierls distortion.

A. J. Heeger, A. G. MacDiarmid, H. Shirakawa, Nobel prize winners in Chemistry, 2000

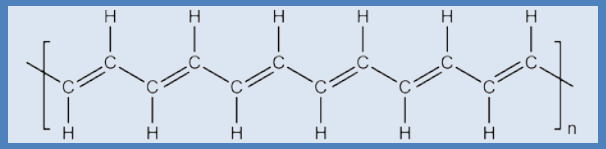

Nanotubes:

superconducting and magnetic instabilities.

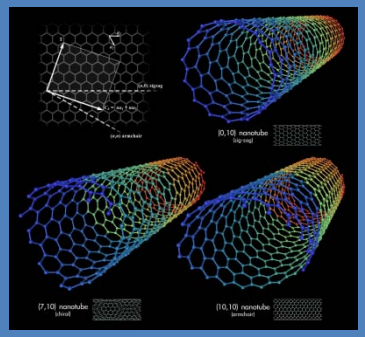

Fullerenes:

superconducting when doped.

R. F. Curl Jr., H. W. Kroto, R. E. Smalley, , Nobel prize winners in Chemistry, 1994

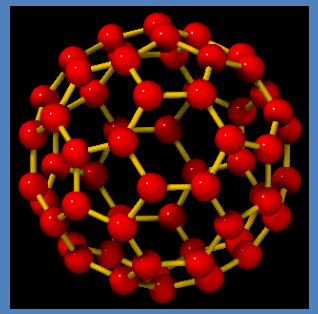

Some early visionaries

The universe (which others call the Library) is composed of an indefinite and perhaps infinite number of hexagonal galleries

The idealists argue that the hexagonal rooms are a necessary form of absolute space or, at least, of our intuition of space. They reason that a triangular or pentagonal room is inconceivable.

The library of Babel, Jorge Luis Borges

Is it not incredible what a pencil has inside it?

Quino

The beginning

Electric Field Effect in Atomically Thin Carbon Films

K. S. Novoselov,[1] A. K. Geim,[1]* S. V. Morozov,[2] D. Jiang,[1] Y. Zhang,[1] S. V. Dubonos,[2] I. V. Grigorieva,[1] A. A. Firsov[2]

We describe monocrystalline graphitic films, which are a few atoms thick but are nonetheless stable under ambient conditions, metallic, and of remarkably high quality. The films are found to be a two-dimensional semimetal with a tiny overlap between valence and conductance bands, and they exhibit a strong ambipolar electric field effect such that electrons and holes in concentrations up to 10^{13} per square centimeter and with room-temperature mobilities of ~10,000 square centimeters per volt-second can be induced by applying gate voltage.

The ability to control electronic properties of a material by externally applied voltage is at the heart of modern electronics. In many cases, it is the electric field effect that allows one to vary the carrier concentration in a semiconductor device and, consequently, change an electric current through it. As the semiconductor industry is nearing the limits of performance improvements for the current technologies dominated by silicon, there is a constant search for new, nontraditional materials whose properties can be controlled by the electric field. The most notable recent examples of such materials are organic conductors (*1*) and carbon nanotubes (*2*). It has long been tempting to extend the use of the field effect to metals [e.g., to develop all-metallic transistors that could be scaled down to much smaller sizes and would consume less energy and operate at higher frequencies than traditional semiconducting devices (*3*)]. However, this would require atomically thin metal films, because the electric field is screened at extremely short distances (<1 nm) and bulk carrier concentrations in metals are large compared to the surface charge that can be induced by the field effect. Films so thin tend to be thermodynamically unstable, becoming discontinuous at thicknesses of several nanometers; so far, this has proved to be an insurmountable obstacle to metallic electronics, and no metal or semimetal has been shown to exhibit any notable (>1%) field effect (*4*).

We report the observation of the electric field effect in a naturally occurring two-dimensional (2D) material referred to as few-layer graphene (FLG). Graphene is the name given to a single layer of carbon atoms densely packed into a benzene-ring structure, and is widely used to describe properties of many carbon-based materials, including graphite, large fullerenes, nanotubes, etc. (e.g., carbon nanotubes are usually thought of as graphene sheets rolled up into nanometer-sized cylinders) (*5–7*). Planar graphene itself has been presumed not to exist in the free state, being unstable with respect to the formation of curved structures such as soot, fullerenes, and nanotubes (*5–14*).

[1]Department of Physics, University of Manchester, Manchester M13 9PL, UK. [2]Institute for Microelectronics Technology, 142432 Chernogolovka, Russia.

*To whom correspondence should be addressed. E-mail: geim@man.ac.uk

Single layer graphene.
Electrically doped.

Two-dimensional atomic crystals

K. S. Novoselov*, D. Jiang*, F. Schedin*, T. J. Booth*, V. V. Khotkevich*, S. V. Morozov†, and A. K. Geim*‡

*Centre for Mesoscience and Nanotechnology and School of Physics and Astronomy, University of Manchester, Manchester M13 9PL, United Kingdom; and †Institute for Microelectronics Technology, Chernogolovka 142432, Russia

Edited by T. Maurice Rice, Swiss Federal Institute of Technology, Zurich, Switzerland, and approved June 7, 2005 (received for review April 6, 2005)

Graphene exfoliation

+

The Big Bang Theory, Feb. 2010

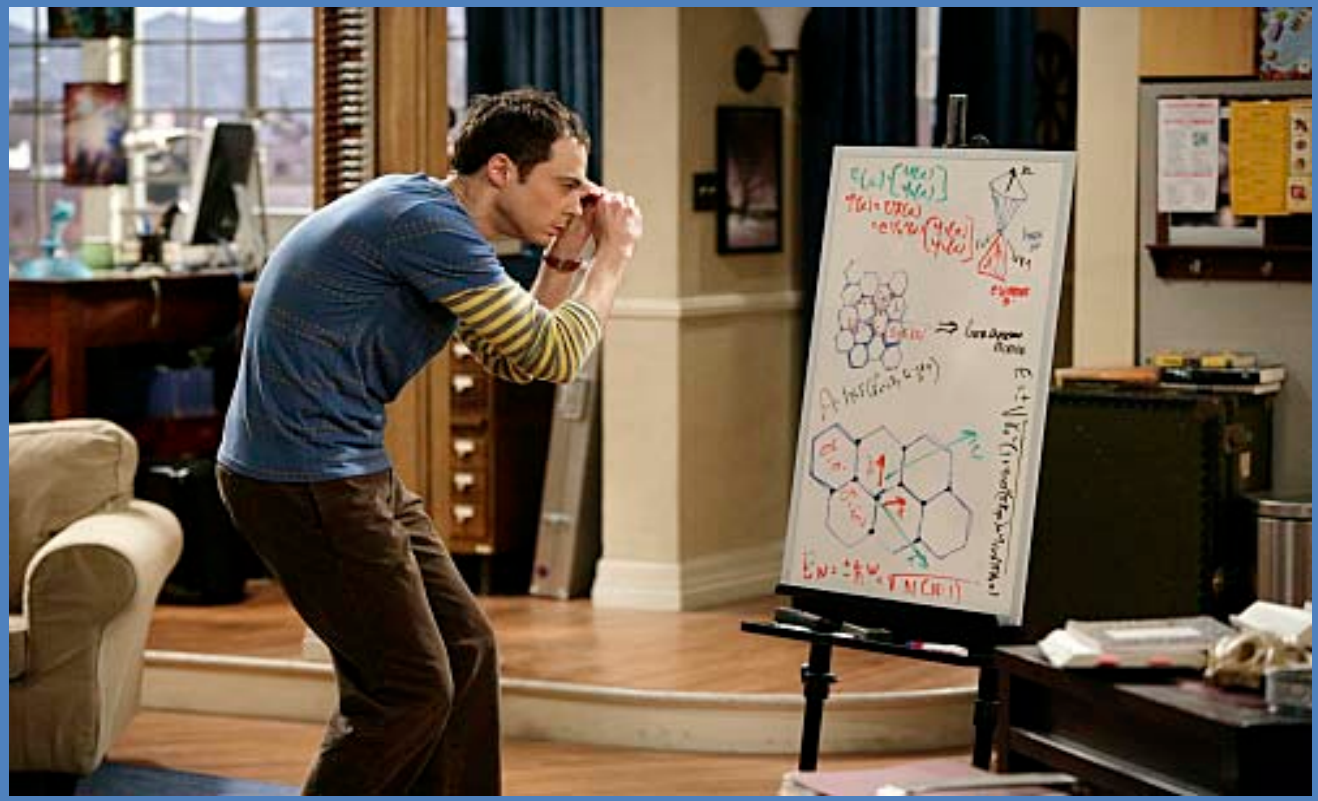

Nobel Symposium, Stockholm, May 2010

Courtesy of M. A. H. Vozmediano

A. K. Geim, interview less than one hour after the announcement

[AS] No, no, it's ok. I mean, for a start, the isolation of graphene using Scotch tape seems beautifully non-Boffin-like and wonderfully accessible. It gives hope to all.

[AG] Yeah, it's a great educational experiment. In a sense not that it's isolation of graphene: it shows people that, in fact, you don't need to be in a Harvard or Cambridge, in one of the universities which collect the smartest people and the best equipment. You can be in the second or even third rated universities in terms of facilities and, whatever, prestige, but you still can do something amazing and something which, I hope, this is an example, which brings more enthusiasm to young generation of inspiring scientists, that they can do something without being at the best place at the best time.
[AS] Hmm, hmm, that's a nice message. The trick in having this approach of playing with new things while finishing off old things must be getting the balance right. You have to learn to find new areas while not neglecting the one's you're working on.

[AG] Yeah, balance is important. And, putting long hours because nothing comes for free. If you ... It's extremely hard, it's extremely hard. First of all, not all the experiments I mentioned – levitating frog, gecko tape, graphene – were originally funded by anyone, ok. And, only graphene later got some research grants to continue this work on another level. But, essentially, you have your work for which you are paid and, yeah, you have not to neglect this work. So, at the same time, you want to start a new subject and, it requires a lot of hours to find the previous literature because, if you are not an expert, you have to look through the literature not to invent the wheel again. And, this is the hardest one.
And, in addition, OK, balance is not as important as courage. Because ... Courage is really important because you stumble on something, ok, which you are still not confident. You feel, ok, sort of you feel secure within your own research area and what you are doing. If you are doing something new, you always can be considered as a fool, inventing the wheel, as I said. Or, you can just be wasting your time. So, the courage is not social courage. The courage is about, ok, investing your time into something which might turn out like a blip.

Graphene is one atom thick

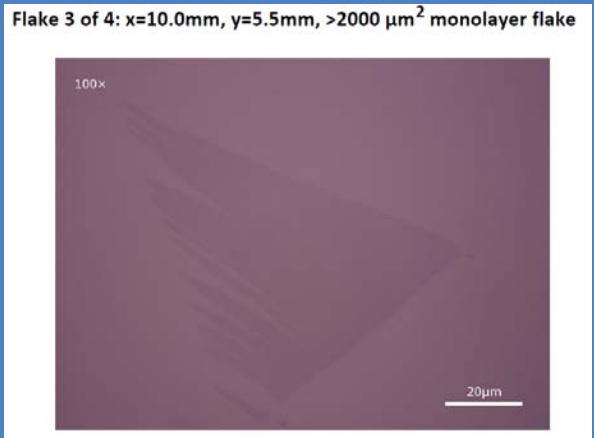

Sample on sale by Graphene Industries, Manchester
Total prize for four flakes: 1.100 £
Approximate prize per gram: 10^{14}€ (EU, USA GDP/yr 1.5×10^{15}€)

Extremely large stiffness
Few defects
Easy to manipulate

Made from only one element, carbon
Robust σ bonds
Four valence electrons

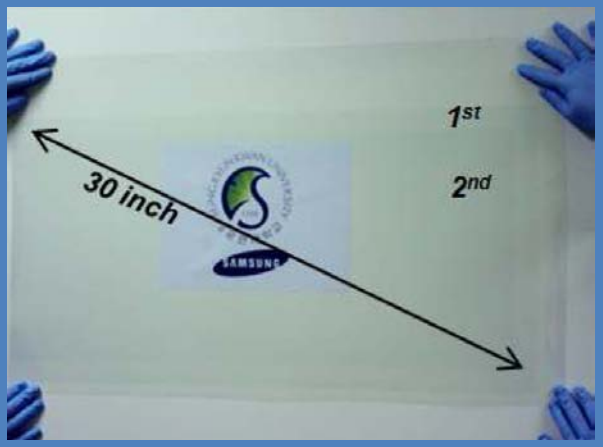

CVD sample from
SKKU, Korea

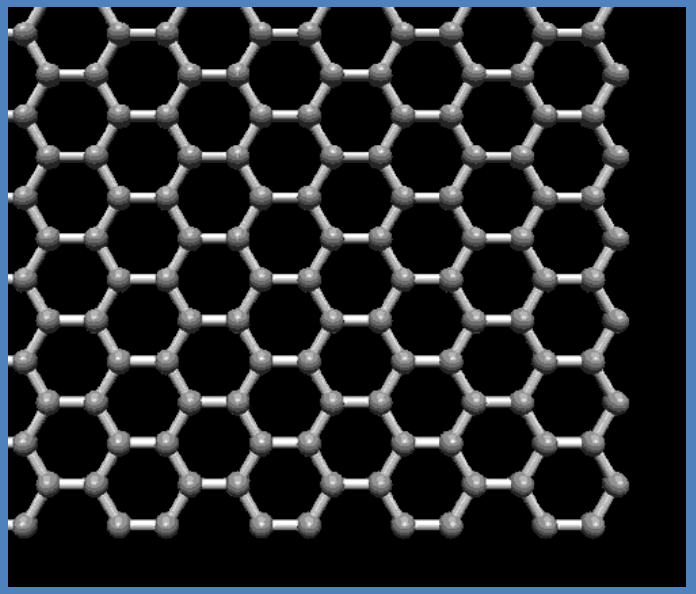

Why are there two dimensional crystals?

STATISTICAL PHYSICS

by

L. D. LANDAU AND E. M. LIFSHITZ

INSTITUTE OF PHYSICAL PROBLEMS,
U.S.S.R. ACADEMY OF SCIENCES

Volume 5 of *Course of Theoretical Physics*

PART 1

THIRD EDITION, REVISED AND ENLARGED
by E. M. LIFSHITZ and L. P. PITAEVSKII

ered). It is easy to see, however, that the thermal fluctuations "smooth out" such a crystal, so that ϱ = constant is the only possibility: the mean

Thermal fluctuations:

$$\langle \vec{u}(L)\vec{u}(0)\rangle \approx \frac{k_B T}{B}\log\left(\frac{L}{d}\right)$$

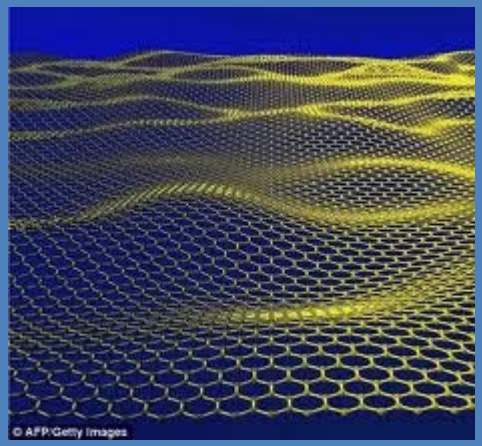

$B_{graphene}$ =22 eV Å^{-2} = 352 N/m

$B_{diamond}$ x d=52.4 N/m

$$T = 300\ K$$

$$L = 1\ Km$$

$$\langle \vec{u}(L)\vec{u}(0)\rangle \approx 0.03\ \overset{0}{\text{A}}$$

Graphene is metallic

Electric Field Effect in Atomically Thin Carbon Films

K. S. Novoselov,[1] A. K. Geim,[1]* S. V. Morozov,[2] D. Jiang,[1] Y. Zhang,[1] S. V. Dubonos,[2] I. V. Grigorieva,[1] A. A. Firsov[2]

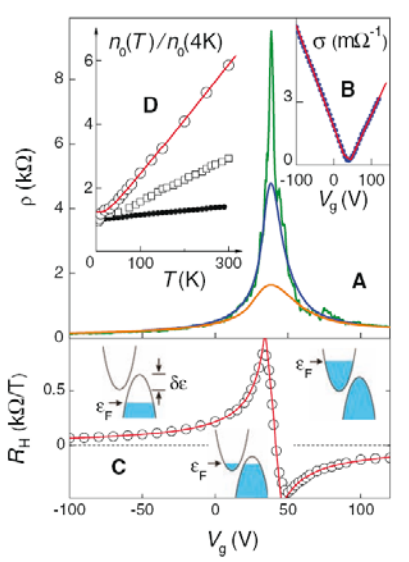

$$\vec{v}_d = \mu \vec{E}$$

μ_{gr} ☮ 30.000 – 1.000.000 $cm^2V^{-1}s^{-1}$

$|n_{min}|$ ≏ 10^8 cm^{-2} , $|n_{max}|$ ♦ 10^{13} cm^{-2}

Typical silicon device at room temperature:

μ_{Si} ☮ 1.400 $cm^2V^{-1}s^{-1}$

Graphene can have electrons or holes

The metallic properties can be varied over a broad range.

Other two dimensional compounds: BN, silicene?

Some basic facts

- Graphene is a membrane one atom thick.
- It is a metal, whose properties can be tuned over a wide range.
- It is the stiffest material known.
- It is chemically inert, and impermeable to all elements.
- The electrons are massless, as in QED.

GRAPHENE'S SUPERLATIVES

- Thinnest imaginable material
- largest surface area (~2,700 m^2 per gram)
- strongest material 'ever measured' (theoretical limit)
- stiffest known material (stiffer than diamond)
- most stretchable crystal (up to 20% elastically)
- record thermal conductivity (outperforming diamond)
- highest current density at room T (106 times of copper)
- completely impermeable (even He atoms cannot squeeze through)
- highest intrinsic mobility (100 times more than in Si)
- conducts electricity in the limit of no electrons
- lightest charge carriers (zero rest mass)
- longest mean free path at room T (micron range)

More novel features

New phases in bilayer graphene
Defects and magnetism
Spin transport, non local effects
Hybrid structures
Graphene plasmonics
Quantum NEMs, FQHE due to strains, …

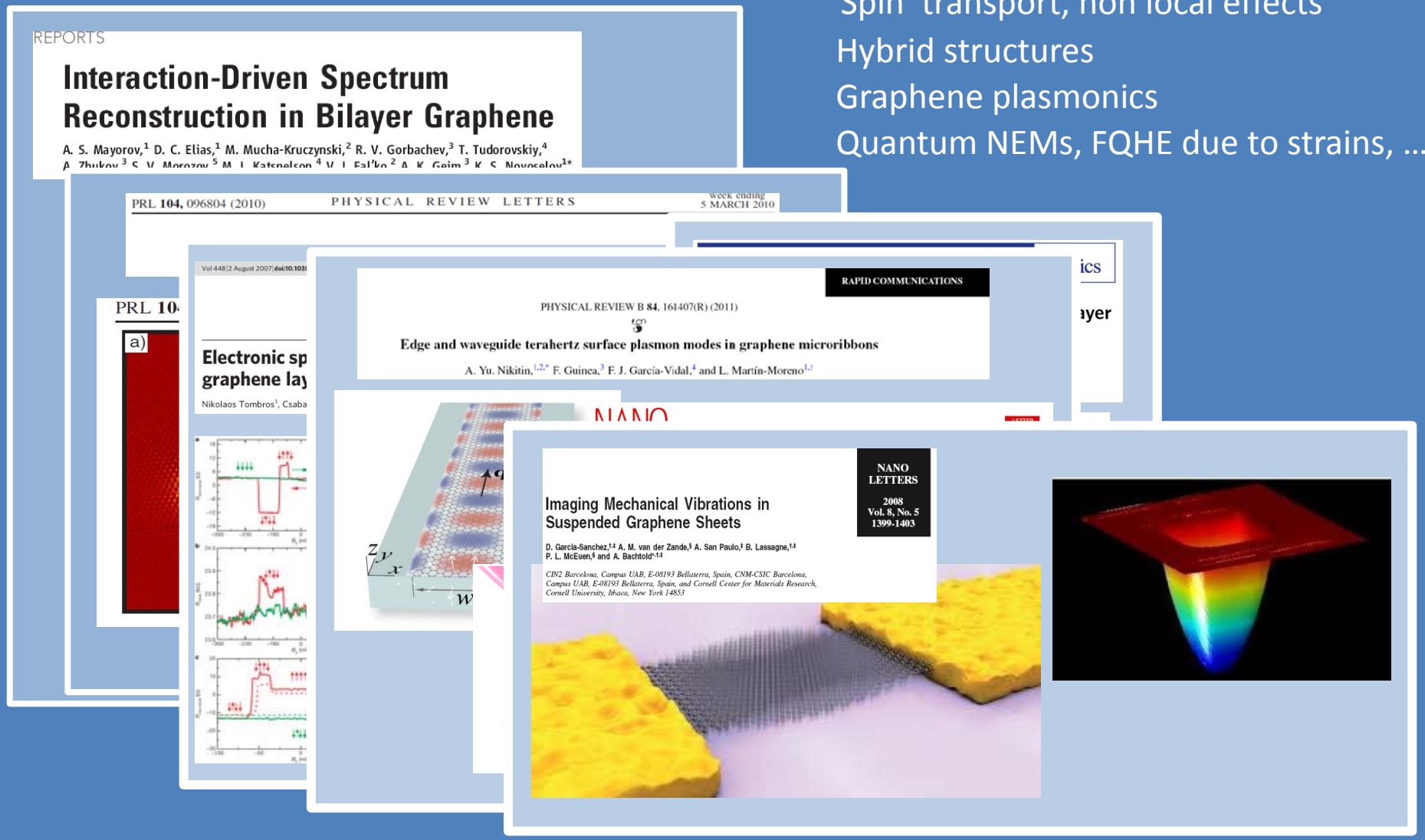

Graphene in the news

Graphene Could Help Physicists Probe the Higgs Boson's Secrets

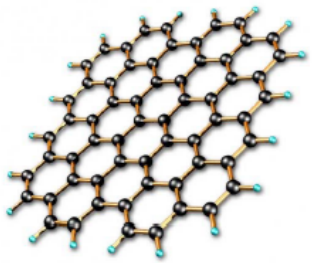

Graphene Sheet Lawrence Berkeley National Laboratory

One of the most promising materials in science could answer some questions about one of the most elusive particles in the universe, according to a new paper. A trio of Spanish physicists believes that graphene, that simple, special Nobel-winning stuff, could provide some key insights into the behavior of the Higgs boson.

When you compress graphene, a one-atom-thick sheet of carbon, it ripples. This is related to the graphene's energy potentials. Spontaneous symmetry breaking — fluctuations that dictate what happens next — cause the ripple effect.

Pablo San-Jose, Francisco Guinea, and Jose Gonzalez at Madrid's Institute for Material Science say this is analogous to the symmetry breaking that happened in a blink after the Big Bang.

In the universe's earliest birth pangs, all four fundamental forces were one, and all was symmetrical with the world. But this hot, dense state was unstable, and as soon as things cooled off, the four forces broke apart into gravity, electromagnetism and the weak and strong nuclear forces.

As Discovery News puts it, this phenomenon is more properly described as the Higgs field (which is associated with the Higgs boson) shifting from a high-energy state to a grounded state. Physics World describes the so-called sombrero effect, or "Mexican hat potentials," in more detail here.

Basically, when graphene responds to being stretched or compressed, the result is similar to what happens when the Higgs field condenses, breaking the symmetry of the universe.

San-Jose says studying the ripple effect of graphene could give hints about the Higgs field and the Higgs boson, which gets its mass from vibrations in the Higgs field. In addition to rippling under pressure, physicists also know that small, spontaneous ripples form in graphene in temperature fluctuations and even without compression.

Now, this does not mean the humble graphene crystal will beat the Large Hadron Collider to a Higgs boson discovery — but it could help physicists work out some of the weird math associated with quantum field theory. That is, if it's even correct. Discovery News talked to one physicist who said the graphene model might not be an accurate representation of how the Higgs field actually works. Still, it's pretty cool — the strongest, thinnest material ever discovered, arguably one of the most important materials in all of science, might help us understand the mechanisms behind the formation of the universe.

[Discovery News]

RELATED ARTICLES

- Nobel Prize In Physics Awarded For Graphene, the Material of the Future
- Strained Graphene Creates Pseudo-Magnetic Fields Stronger Than Any Before Seen
- In Stores Soon: Graphene-Enhanced Lithium Batteries That Charge In Minutes

TAGS

Technology, Rebecca Boyle, big bang, graphene, Higgs boson, mathematical symmetry, particle physics, physics, quantum field, quantum mechanics

---

ZDNet UK / Blogs / Qubits and Pieces

Fastest transistor yet boosts graphene's super-status

By Lucy Sherriff , 4 February, 2011 14:56

About this blog

Qubits and Pieces

News from the frontline of the weird and wonderful world of quantum computing. From the theoretical musings of solid state physicists to breakthroughs you might actually see in a data centre in your l… Read more »ifetime, we'll be keeping an eye on stuff that matters in materials science, including graphene, condensed matter, diamonds and so on. And last, but by no mean least, we'll be tracking the spin on spintronics. Just don't mention

---

BLOGS // NANOCLAST

Graphene or Molybdenite? Which Replaces Silicon in the Transistor of the Future?

POSTED BY: DEXTER JOHNSON / MIÉ, FEBRERO 02, 2011

Graphene seems to be winning fans, awards and application possibilities seemingly daily. But the elephant in the room, if you will, when discussing graphene, is the problem of it lacking a band gap.

Huge strides have been made in overcoming that shortcoming, but let's just say that not having a band gap in its nature is more than a small liability for graphene in electronic applications.

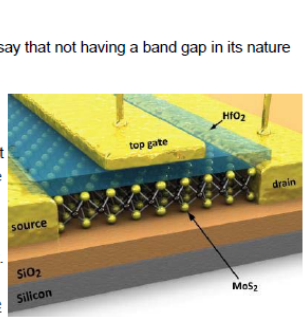

Into this mix, researchers at Ecole Polytechnique Federale de Lausanne's (EPFL) Laboratory of Nanoscale Electronics and Structures (LANES) had their research published this week in the journal *Nature Nanotechnology* that offers the humble and abundant mineral molybdenite (MoS2) as an attractive alternative to silicon as a two-dimensional material (like graphene is) for replacing the three-dimensional silicon in transistors.

"It's a two-dimensional material, very thin and easy to use in nanotechnology. It has real potential in the fabrication of very small transistors, light-emitting diodes (LEDs) and solar cells," says EPFL Professor Andras Kis in an article that reports on the research.

The big advantage it has over graphene in the search for a replacement to silicon: it has a band gap. And when it comes to being better than silicon, the advantages are impressive.

The Dirac equation

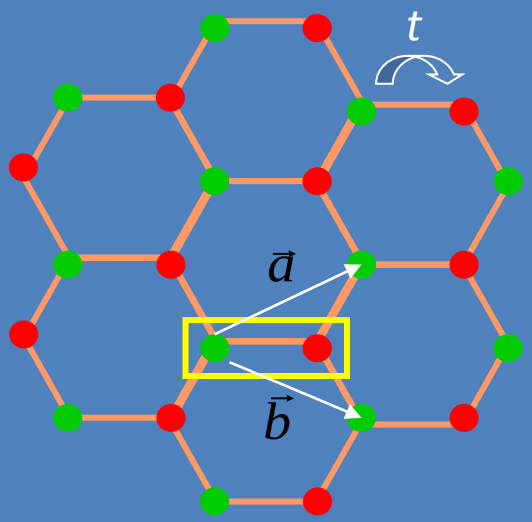

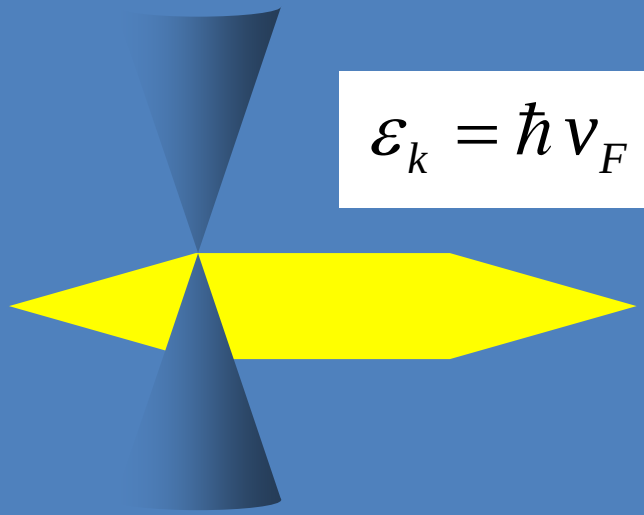

$$\varepsilon_k = \hbar v_F k$$

$$H \cong \frac{3ta}{2}\begin{pmatrix} 0 & k_x + ik_y \\ k_x - ik_y & 0 \end{pmatrix}$$

Density of states

$$D(E) = \frac{2E}{\pi \hbar^2 v_F^2}$$

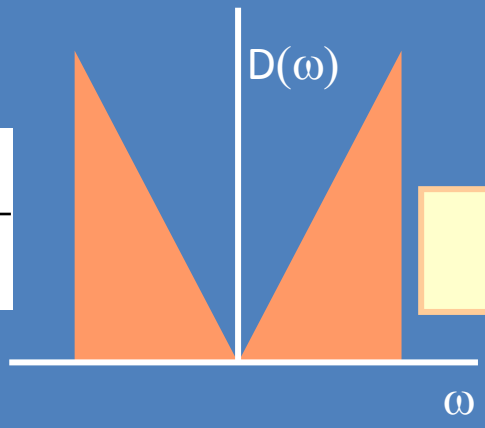

Graphene is a semimetal

No metallic screening.
Logarithmic divergences, as in QED

Ripples in graphene

nature

Vol 446|1 March 2007|doi:10.1038/nature05545

LETTERS

The structure of suspended graphene sheets

Jannik C. Meyer[1], A. K. Geim[2], M. I. Katsnelson[3], K. S. Novoselov[2], T. J. Booth[2] & S. Roth[1]

Figure 1 | Suspended graphene membrane. Bright-field TEM image of a suspended graphene membrane. Its central part (homogeneous and featureless region indicated by arrows) is monolayer graphene. Electron diffraction images from different areas of the flake show that it is a single crystal without domains. We note scrolled top and bottom edges and a strongly folded region on the right. Scale bar, 500 nm.

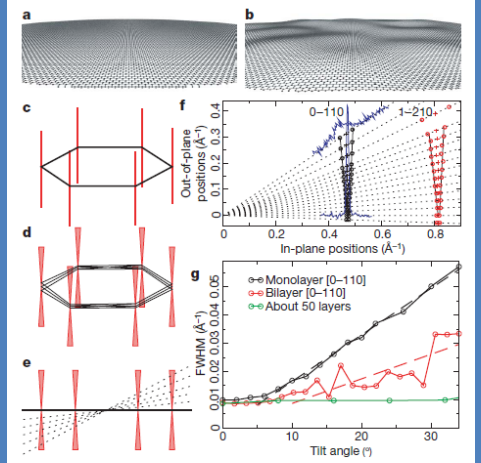

Figure 3 | Microscopically corrugated graphene. **a**, Flat graphene crystal in real space (perspective view). **b**, The same for corrugated graphene. The roughness shown imitates quantitatively the roughness found experimentally. **c**, The reciprocal space for a flat sheet is a set of rods (red) directed perpendicular to the reciprocal lattice of graphene (black hexagon). **d**, **e**, For the corrugated sheet, a superposition of the diffracting beams from microscopic flat areas effectively turns the rods into cone-shaped volumes so that diffraction spots become blurred at large angles (indicated by the dotted lines in **e**) and the effect is more pronounced further away from the tilt axis (compare with Fig. 2). Diffraction patterns obtained at different tilt angles allow us to measure graphene roughness. **f**, Evolution of diffraction peaks with tilt angle in monolayer graphene. The experimental data are presented in such a way that they closely resemble the schematic view in **e**. For each tilt angle, the black dotted line represents a cross-section for diffraction peaks (0–110) and (1–210). The peak centres and full widths at half maxima (FWHM) in reciprocal space are marked by crosses and open circles, respectively. In two cases (0° and 34°), the recorded intensities are shown in full by blue curves. All the intensity curves could be well fitted by the gaussian shape. The solid black lines show that the width of the diffraction spots reproduces the conical broadening suggested by our model (**d** and **e**). **g**, FWHM for the (0–110) diffraction peak in monolayer and bilayer membranes and thin graphite (as a reference), as a function of tilt angle. The dashed lines are the linear fits yielding the average roughness. The flat region between 0° to 5°, and also for the reference sample, is due to the intrinsic peak width for the microscope at our settings.

Ripples in graphene

Scattering and Interference in Epitaxial Graphene

G. M. Rutter,[1] J. N. Crain,[2] N. P. Guisinger,[2] T. Li,[1] P. N. First,[1]* J. A. Stroscio[2]*

A single sheet of carbon, graphene, exhibits unexpected electronic properties that arise from quantum state symmetries, which restrict the scattering of its charge carriers. Understanding the role of defects in the transport properties of graphene is central to realizing future electronics based on carbon. Scanning tunneling spectroscopy was used to measure quasiparticle interference patterns in epitaxial graphene grown on SiC(0001). Energy-resolved maps of the local density of states reveal modulations on two different length scales, reflecting both intravalley and intervalley scattering. Although such scattering in graphene can be suppressed because of the symmetries of the Dirac quasiparticles, we show that, when its source is atomic-scale lattice defects, wave functions of different symmetries can mix.

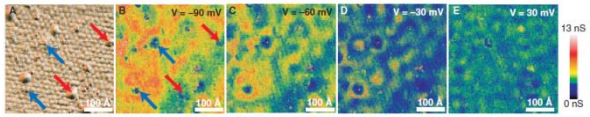

Fig. 2. Defect scattering in bilayer epitaxial graphene. (**A**) STM topography and (**B** to **E**) simultaneously acquired spectroscopic *dI*/*dV* maps. Type A defects (mounds) and type B defects are labeled with red and blue arrows, respectively. Sample biases are: (B) −90 mV, (C) −60 mV, (D) −30 mV, and (E) 30 mV. $I = 500$ pA, $V = 100$ mV, $\Delta V = 1$ mV$_{rms}$ where ΔV is the modulation voltage.

High-resolution scanning tunneling microscopy imaging of mesoscopic graphene sheets on an insulating surface

Elena Stolyarova†, Kwang Taeg Rim†, Sunmin Ryu†, Janina Maultzsch‡, Philip Kim‡, Louis E. Brus†, Tony F. Heinz‡, Mark S. Hybertsen§, and George W. Flynn†¶

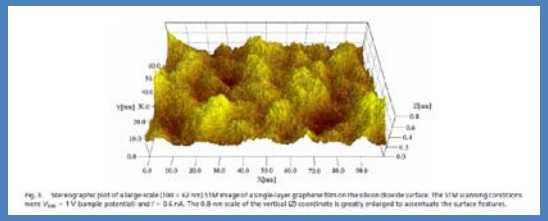

Fig. 3. Stereographic plot of a large-scale (100 × 42 nm) STM image of a single-layer graphene film on the silicon dioxide surface. The STM scanning conditions were $V_{bias} = 1$ V (sample potential) and $I = 0.6$ nA. The 0.8 nm scale of the vertical (Z) coordinate is greatly enlarged to accentuate the surface features.

PRL 101, 206802 (2008) PHYSICAL REVIEW LETTERS week ending 14 NOVEMBER 2008

Quasiparticle Chirality in Epitaxial Graphene Probed at the Nanometer Scale

I. Brihuega,[1] P. Mallet,[2,*] C. Bena,[3] S. Bose,[1] C. Michaelis,[1] L. Vitali,[1] F. Varchon,[2] L. Magaud,[2] K. Kern,[1,4] and J.-Y. Veuillen[2]

[1]*Max-Planck-Institut für Festkörperforschung, Heisenbergstrasse 1, D-70569 Stuttgart, Germany*
[2]*Institut Néel, CNRS-UJF, BP166, 38042 Grenoble, France*
[3]*Institut de Physique Théorique, CEA/Saclay, Orme des Merisiers, 91190 Gif-sur-Yvette, France*
[4]*Institut de Physique des Nanostructures, Ecole Polytechnique Fédérale de Lausanne, CH-1015 Lausanne, Switzerland*

(Received 27 May 2008; published 14 November 2008)

Graphene exhibits unconventional two-dimensional electronic properties resulting from the symmetry of its quasiparticles, which leads to the concepts of pseudospin and electronic chirality. Here, we report that scanning tunneling microscopy can be used to probe these unique symmetry properties at the nanometer scale. They are reflected in the quantum interference pattern resulting from elastic scattering off impurities, and they can be directly read from its fast Fourier transform. Our data, complemented by theoretical calculations, demonstrate that the pseudospin and the electronic chirality in epitaxial graphene on SiC(0001) correspond to the ones predicted for ideal graphene.

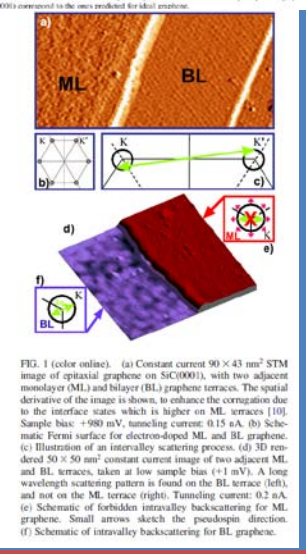

FIG. 1 (color online). (a) Constant current 90 × 43 nm² STM image of epitaxial graphene on SiC(0001), with two adjacent monolayer (ML) and bilayer (BL) graphene terraces. The spatial derivative of the image is shown, to enhance the corrugation due to the interface states which is higher on ML terraces [10]. Sample bias: +980 mV, tunneling current: 0.15 nA. (b) Schematic Fermi surface for electron-doped ML and BL graphene. (c) Illustration of an intervalley scattering process. (d) 3D rendered 50 × 50 nm² constant current image of two adjacent ML and BL terraces, taken at low sample bias (+1 mV). A long wavelength scattering pattern is found on the BL terrace (left), and not on the ML terrace (right). Tunneling current: 0.2 nA. (e) Schematic of forbidden intravalley backscattering for ML graphene. Small arrows sketch the pseudospin direction. (f) Schematic of intravalley backscattering for BL graphene.

PRL 100, 056807 (2008) PHYSICAL REVIEW LETTERS week ending 8 FEBRUARY 2008

Periodically Rippled Graphene: Growth and Spatially Resolved Electronic Structure

A. L. Vázquez de Parga,[1] F. Calleja,[1] B. Borca,[1] M. C. G. Passeggi, Jr.,[2] J. J. Hinarejos,[1] F. Guinea,[3] and R. Miranda[1,4]

[1]*Departamento de Física de la Materia Condensada e Instituto Nicolás Cabrera, Universidad Autónoma de Madrid, Cantoblanco, 28049 Madrid, Spain*
[2]*Laboratorio de Superficies e Interfases, INTEC (CONICET and UNL), S3000GLN Santa Fe, Argentina*
[3]*Instituto de Ciencia de Materiales, Consejo Superior de Investigaciones Científicas, Cantoblanco, 28049 Madrid, Spain*
[4]*Instituto Madrileño de Estudios Avanzados en Nanociencia (IMDEA Nanociencia), Cantoblanco, 28049 Madrid, Spain*

(Received 10 August 2007; published 7 February 2008)

We grow epitaxial graphene monolayers on Ru(0001) that cover uniformly the substrate over lateral distances larger than several microns. The weakly coupled graphene monolayer is periodically rippled and it shows charge inhomogeneities in the charge distribution. Real space measurements by scanning tunneling spectroscopy reveal the existence of electron pockets at the higher parts of the ripples, as predicted by a simple theoretical model. We also visualize the geometric and electronic structure of edges of graphene nanoislands.

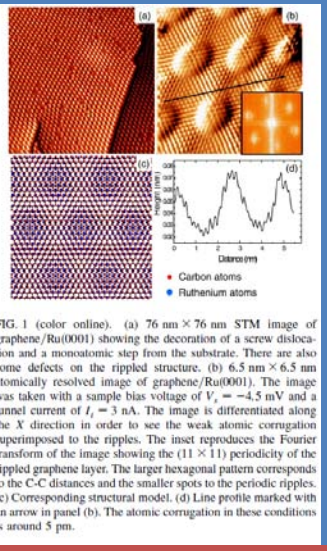

FIG. 1 (color online). (a) 76 nm × 76 nm STM image of graphene/Ru(0001) showing the decoration of a screw dislocation and a monoatomic step from the substrate. There are also some defects on the rippled structure. (b) 6.5 nm × 6.5 nm atomically resolved image of graphene/Ru(0001). The image was taken with a sample bias voltage of $V_s = -4.5$ mV and a tunnel current of $I_t = 3$ nA. The image is differentiated along the X direction in order to see the weak atomic corrugation superimposed to the ripples. The inset reproduces the Fourier transform of the image showing the (11 × 11) periodicity of the rippled graphene layer. The larger hexagonal pattern corresponds to the C-C distances and the smaller spots to the periodic ripples. (c) Corresponding structural model. (d) Line profile marked with an arrow in panel (b). The atomic corrugation in these conditions is around 5 pm.

NANO LETTERS 2007 Vol. 7, No. 6 1643-1648

Atomic Structure of Graphene on SiO_2

Masa Ishigami,[†,‡] J. H. Chen,[†] W. G. Cullen,[†] M. S. Fuhrer,[†,§] and E. D. Williams[†]*

Materials Research Science and Engineering Center, Department of Physics, and Center for Superconductivity Research, University of Maryland, College Park, Maryland 20742

Received March 14, 2007; Revised Manuscript Received April 10, 2007

ABSTRACT

We employ scanning probe microscopy to reveal atomic structures and nanoscale morphology of graphene-based electronic devices (i.e., a graphene sheet supported by an insulating silicon dioxide substrate) for the first time. Atomic resolution scanning tunneling microscopy images reveal the presence of a strong spatially dependent perturbation, which breaks the hexagonal lattice symmetry of the graphitic lattice. Structural corrugations of the graphene sheet partially conform to the underlying silicon oxide substrate. These effects are obscured or modified on graphene devices processed with normal lithographic methods, as they are covered with a layer of photoresist residue. We enable our experiments by a novel cleaning process to produce atomically clean graphene sheets.

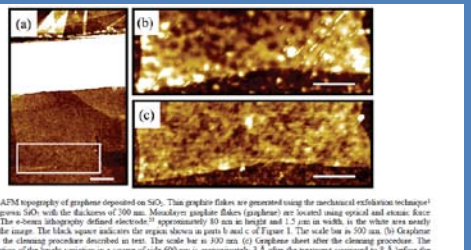

Figure 2. (a) AFM topography of graphene deposited on SiO_2. Thin graphite flakes are generated using the mechanical exfoliation technique[1] on thermally grown SiO_2 with the thickness of 300 nm. Monolayers (graphene flakes (graphene) are located using optical and atomic force microscopy.[1] The e-beam lithography defined electrodes[23] approximately 80 nm in height and 1.5 μm in width, is the white area nearly horizontal to the image. The black square indicates the region shown in parts b and c of Figure 1. The scale bar is 500 nm. (b) Graphene sheet prior to the cleaning procedure described in text. The scale bar is 300 nm. (c) Graphene sheet after the cleaning procedure. The standard deviations of the height variation in a square of side 600 nm is approximately 3 Å after the treatment compared to 8 Å before the treatment. The scale bar is 300 nm. Images a−c were acquired using intermittent-contact mode AFM in air.

PRL 102, 076102 (2009) PHYSICAL REVIEW LETTERS week ending 20 FEBRUARY 2009

Intrinsic and extrinsic corrugation of monolayer graphene deposited on SiO_2

V. Geringer,[1,2] M. Liebmann,[1,2] T. Echtermeyer,[2] S. Runte,[1,2] M. Schmidt,[1,2] R. Rückamp,[1,2] M. C. Lemme,[2] and M. Morgenstern[1,2]

[1]*II. Institute of Physics, RWTH Aachen University, Otto-Blumenthal-Straße, 52074 Aachen, Germany*
[2]*Advanced Microelectronic Center Aachen (AMICA), AMO GmbH, Otto-Blumenthal-Straße 25, 52074 Aachen, Germany*
[3]*JARA: Fundamentals of Future Information Technology, Otto-Blumenthal-Straße, 52074 Aachen, Germany*

(Received 5 June 2008; published 17 February 2009)

Using scanning tunneling microscopy in an ultrahigh vacuum and atomic force microscopy, we investigate the corrugation of graphene flakes deposited by exfoliation on a Si/SiO_2 (300 nm) surface. While the corrugation on SiO_2 is long range with a correlation length of about 25 nm, some of the graphene monolayers exhibit an additional corrugation with a preferential wavelength of about 15 nm. A detailed analysis shows that the long-range corrugation of the substrate is also visible on graphene, but with a reduced amplitude, leading to the conclusion that the graphene is partly freely suspended between hills of the substrate. Thus, the intrinsic rippling observed previously on artificially suspended graphene can exist as well, if graphene is deposited on SiO_2.

DOI: 10.1103/PhysRevLett.102.076102 PACS numbers: 68.55.J−, 68.37.Ef, 68.37.Ps, 68.65.−k

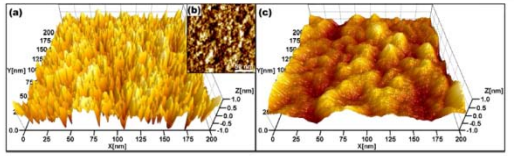

FIG. 3 (color online). (a), (b) 3D and 2D constant current STM image of monolayer graphene (1 V, 207 pA). (c) 3D tapping mode AFM image of the SiO_2 substrate (resonance frequency 326.4 kHz, force constant 47 N/m, excitation frequency 326.5 kHz, oscillation amplitude 18 nm, constant amplitude feedback, set point 90%). Note the identical scale of both images.

Elastic properties of graphene

Measurement of the Elastic Properties and Intrinsic Strength of Monolayer Graphene

Changgu Lee,[1,2] Xiaoding Wei,[1] Jeffrey W. Kysar,[1,3] James Hone[1,2,4]*

We measured the elastic properties and intrinsic breaking strength of free-standing monolayer graphene membranes by nanoindentation in an atomic force microscope. The force-displacement behavior is interpreted within a framework of nonlinear elastic stress-strain response, and yields second- and third-order elastic stiffnesses of 340 newtons per meter (N m^{-1}) and −690 N m^{-1}, respectively. The breaking strength is 42 N m^{-1} and represents the intrinsic strength of a defect-free sheet. These quantities correspond to a Young's modulus of E = 1.0 terapascals, third-order elastic stiffness of D = −2.0 terapascals, and intrinsic strength of σ_{int} = 130 gigapascals for bulk graphite. These experiments establish graphene as the strongest material ever measured, and show that atomically perfect nanoscale materials can be mechanically tested to deformations well beyond the linear regime.

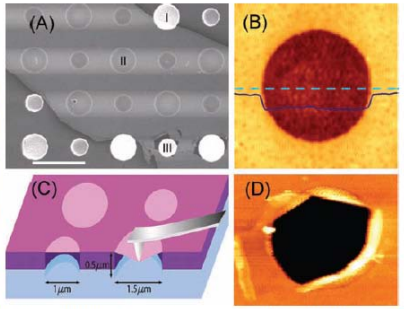

Fig. 1. Images of suspended graphene membranes. **(A)** Scanning electron micrograph of a large graphene flake spanning an array of circular holes 1 μm and 1.5 μm in diameter. Area I shows a hole partially covered by graphene, area II is fully covered, and area III is fractured from indentation. Scale bar, 3 μm. **(B)** Noncontact mode AFM image of one membrane, 1.5 μm in diameter. The solid blue line is a height profile along the dashed line. The step height at the edge of the membrane is about 2.5 nm. **(C)** Schematic of nanoindentation on suspended graphene membrane. **(D)** AFM image of a fractured membrane.

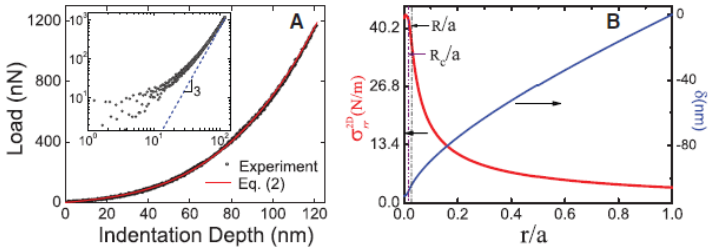

Fig. 2. **(A)** Loading/unloading curve and curve fitting to Eq. 2. The curve approaches cubic behavior at high loads (inset). **(B)** Maximum stress and deflection of graphene membrane versus normalized radial distance at maximum loading (simulation based on nonlinear elastic behavior in Eq. 1). The dashed lines indicate the tip radius R and contact radius R_c.

nature Vol 457|5 February 2009|doi:10.1038/nature07719

LETTERS

Large-scale pattern growth of graphene films for stretchable transparent electrodes

Keun Soo Kim[1,3,4], Yue Zhao[7], Houk Jang[2], Sang Yoon Lee[5], Jong Min Kim[5], Kwang S. Kim[6], Jong-Hyun Ahn[2,3], Philip Kim[3,7], Jae-Young Choi[5] & Byung Hee Hong[1,3,4]

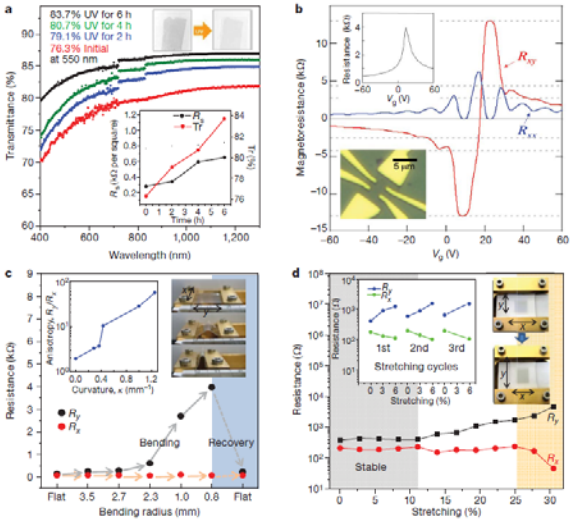

Figure 4 | Optical and electrical properties of the graphene films. **a**, Transmittance of the graphene films on a quartz plate. The discontinuities in the absorption curves arise from the different sensitivities of the switching detectors. The upper inset shows the ultraviolet (UV)-induced thinning and the consequent enhancement of transparency. The lower inset shows the changes in transmittance, Tr, and sheet resistance, R_s, as functions of ultraviolet illumination time. **b**, Electrical properties of monolayer graphene devices showing the half-integer quantum Hall effect and high electron mobility. The upper inset shows a four-probe electrical resistance measurement on a monolayer graphene Hall bar device (lower inset) at 1.6 K. We apply a gate voltage, V_g, to the silicon substrate to control the charge density in the graphene sample. The main panel shows longitudinal (R_{xx}) and transverse (R_{xy}) magnetoresistances measured in this device for a magnetic field B = 8.8 T. The monolayer graphene quantum Hall effect is clearly observed, showing the plateaux with filling factor $\nu = 2$ at $R_{xy} = (2e^2/h)^{-1}$ and zeros in R_{xx}. (Here e is the elementary charge and h is Planck's constant.) Quantum Hall plateaux (horizontal dashed lines) are developing for higher filling factors. **c**, Variation in resistance of a graphene film transferred to a ~0.3-mm-thick PDMS/PET substrate for different distances between holding stages (that is, for different bending radii). The left inset shows the anisotropy in four-probe resistance, measured as the ratio, R_y/R_x, of the resistances parallel and perpendicular to the bending direction, y. The right inset shows the bending process. **d**, Resistance of a graphene film transferred to a PDMS substrate isotropically stretched by ~12%. The left inset shows the case in which the graphene film is transferred to an unstretched PDMS substrate. The right inset shows the movement of holding stages and the consequent change in shape of the graphene film.

Elastic properties of graphene

NANO LETTERS
2008
Vol. 8, No. 8
2458-2462

Impermeable Atomic Membranes from Graphene Sheets

J. Scott Bunch, Scott S. Verbridge, Jonathan S. Alden, Arend M. van der Zande, Jeevak M. Parpia, Harold G. Craighead, and Paul L. McEuen*

Cornell Center for Materials Research, Cornell University, Ithaca, New York 14853

Received May 21, 2008; Revised Manuscript Received June 12, 2008

ABSTRACT

We demonstrate that a monolayer graphene membrane is impermeable to standard gases including helium. By applying a pressure difference across the membrane, we measure both the elastic constants and the mass of a single layer of graphene. This pressurized graphene membrane is the world's thinnest balloon and provides a unique separation barrier between 2 distinct regions that is only one atom thick.

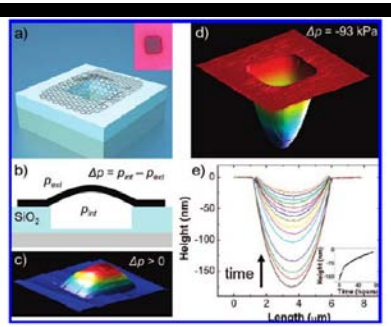

Figure 1. (a) Schematic of a graphene sealed microchamber. (Inset) optical image of a single atomic layer graphene drumhead on 440 nm of SiO_2. The dimensions of the microchamber are 4.75 μm × 4.75 μm × 380 nm. (b) Side view schematic of the graphene sealed microchamber. (c) Tapping mode atomic force microscope (AFM) image of a ~ 9 nm thick many layer graphene drumhead with $\Delta p > 0$. The dimensions of the square microchamber are 4.75 μm × 4.75 μm. The upward deflection at the center of the membrane is $z = 90$ nm. (d) AFM image of the graphene sealed microchamber of Figure 1a with $\Delta p = -93$ kPa across it. The minimum dip in the z direction is 175 nm. (e) AFM line traces taken through the center of the graphene membrane of (a). The images were taken continuously over a span of 71.3 h and in ambient conditions. (Inset) deflection at the center of the graphene membrane vs time. The first deflection measurement ($z = 175$ nm) is taken 40 min after removing the microchamber from vacuum.

***Nature Nanotechnology* 4**, 562 - 566 (2009)
Published online: 26 July 2009 | **doi:10.1038/nnano.2009.191**
Subject Categories: Nanomaterials | Structural properties

Controlled ripple texturing of suspended graphene and ultrathin graphite membranes

Wenzhong Bao1, Feng Miao1, Zhen Chen2, Hang Zhang1, Wanyoung Jang2, Chris Dames2 & Chun Ning Lau1

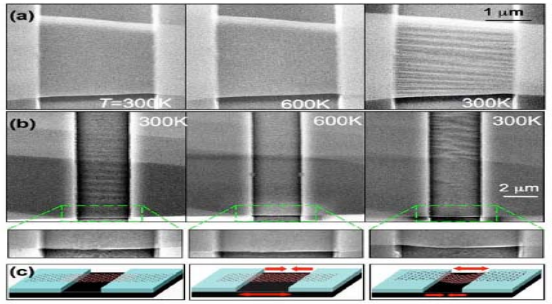

Graphene admits large strains, at least 10%
Strains can be controlled
Graphene seems to have few defects
Open questions: melting, wrinkles, mechanical instabilities?

Lattice frustration as a gauge potential.

J. González, F. G. and M. A. H. Vozmediano, Phys. Rev. Lett. **69**, 172 (1992)

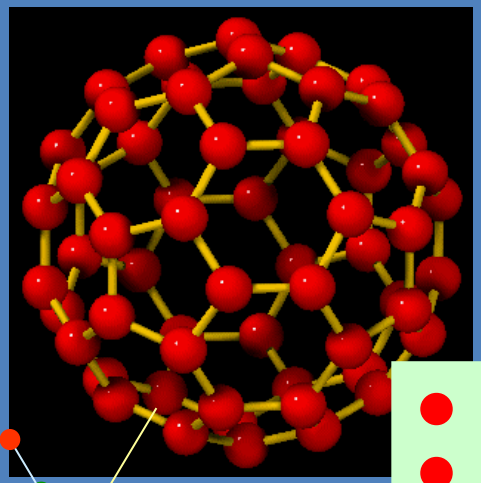

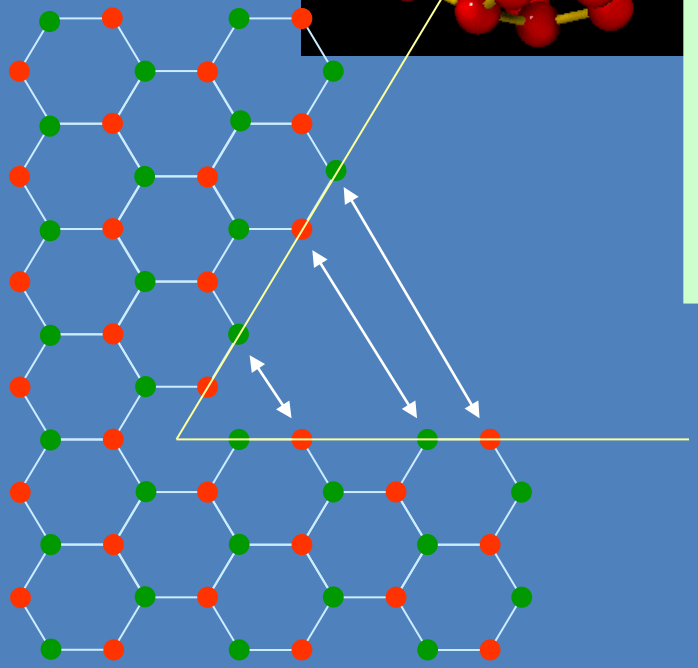

- **A fivefold ring defines a disclination.**
- **The sublattices are interchanged.**
- **The Fermi points are also interchanged.**
- **These transformations can be achieved by means of a gauge potential.**

$$i\vec{\nabla} \rightarrow i\vec{\nabla} - \vec{A}\begin{pmatrix} 0 & 1 \\ 1 & 0 \end{pmatrix}$$

$$\Phi = \int \vec{A}\, d\vec{l}$$

The flux Φ is determined by the total rotation induced by the defect.

Continuum model of the fullerenes.

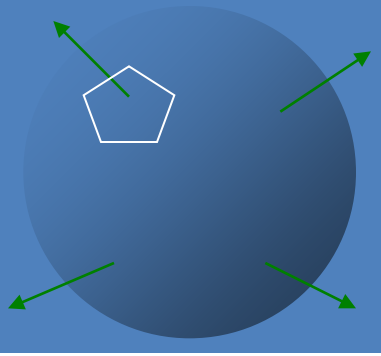

- Dirac equation on a spherical surface.
- Constant magnetic field (Dirac monopole).

$$\frac{\hbar v_F}{R}\left[i\partial_\theta - \frac{1}{\sin(\theta)}\partial_\phi + \frac{i(1+l)\cos(\theta)}{2\sin(\theta)}\right]\Psi_a = \varepsilon\Psi_b$$

$$\frac{\hbar v_F}{R}\left[i\partial_\theta + \frac{1}{\sin(\theta)}\partial_\phi + \frac{i(1-l)\cos(\theta)}{2\sin(\theta)}\right]\Psi_b = \varepsilon\Psi_a$$

$$\varepsilon_J = \frac{\hbar v_F}{R}\sqrt{\left[J(J+1)\right] - \frac{l^2-1}{4}} \qquad J \geq \left|\frac{l-1}{2}\right|$$

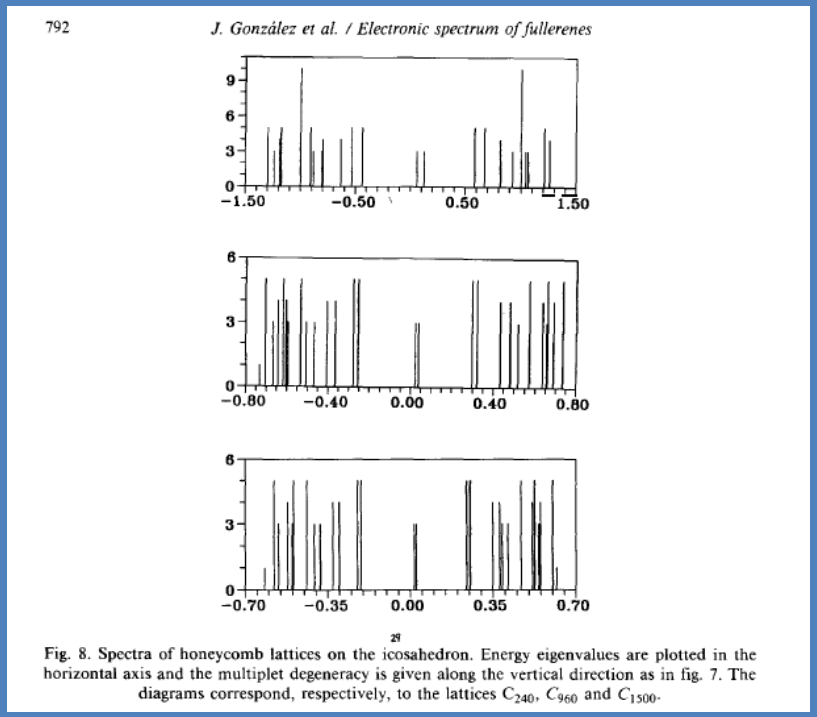
792 J. González et al. / Electronic spectrum of fullerenes

Fig. 8. Spectra of honeycomb lattices on the icosahedron. Energy eigenvalues are plotted in the horizontal axis and the multiplet degeneracy is given along the vertical direction as in fig. 7. The diagrams correspond, respectively, to the lattices C_{240}, C_{960} and C_{1500}.

J. González, F. G., and M. A. H. Vozmediano, Nucl. Phys.B 406, 771 (1993)

Effective gauge fields

$$H \equiv \begin{pmatrix} 0 & t_1 e^{i\vec{k}_1\vec{a}_1} + t_2 e^{i\vec{k}_2\vec{a}_2} + t_3 e^{i\vec{k}_3\vec{a}_3} \\ t_1 e^{-i\vec{k}_1\vec{a}_1} + t_2 e^{-i\vec{k}_2\vec{a}_2} + t_3 e^{-i\vec{k}_3\vec{a}_3} & 0 \end{pmatrix} \approx \begin{pmatrix} 0 & \frac{3\bar{t}a}{2}\left(k_x + ik_y\right) + \Delta t \\ \frac{3\bar{t}a}{2}\left(k_x + ik_y\right) + \Delta t & 0 \end{pmatrix}$$

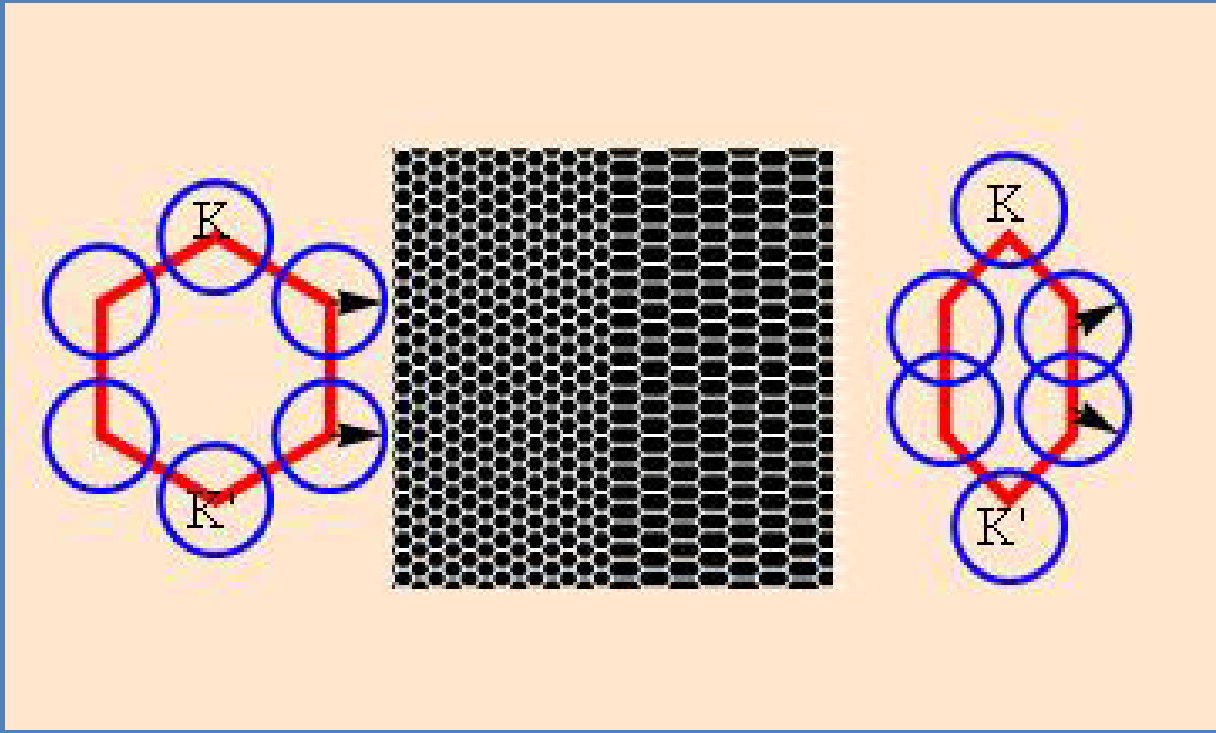

A modulation of the hoppings leads to a term which modifies the momentum: an effective gauge field.

The induced “magnetic” fields have opposite sign at the two corners of the Brillouin Zone.

Effective gauge fields

$$K_{xxx} = 1$$
$$K_{xxy} = K_{xyx} = K_{yxx} = -1$$
$$A_i = c\,K_{ijk}u_{kl}$$

$$A_x = \frac{\beta}{a}\left(u_{xx} - u_{yy}\right)$$

$$A_y = \frac{2\beta}{a}u_{xy}$$

$$\beta = \frac{\partial \log(t)}{\partial \log(a)} \approx 2$$

H. Suzuura and T. Ando, Phys. Rev. B **65**, 235412 (2002)
J. L. Mañes, Phys. Rev. B **76**, 045430 (2007)
M. A. H. Vozmediano, M. I. Katsnelson, F. G., arXiv:1003.5179 (2010), Physics Reports **496**, 109 (2010)

- The effective gauge field can be obtained from the strain tensor
- It reflects the trigonal symmetry of the honeycomb lattice
- It depends on the electron-phonon coupling, β

Resistivity due to acoustical phonons

Scalar potential

Gauge potential

$$H_D^{K,K'} \equiv \begin{pmatrix} g\left(u_{xx}+u_{yy}\right) & v_F\left(\pm i\partial_x+\partial_y\right)+\beta t\left(u_{xx}-u_{yy}\pm 2iu_{xy}\right) \\ v_F\left(\pm i\partial_x-\partial_y\right)+\beta t\left(u_{xx}-u_{yy}\mp 2iu_{xy}\right) & g\left(u_{xx}+u_{yy}\right) \end{pmatrix}$$

$$\rho \approx \frac{\hbar}{e^2}\left(g^2+\frac{\hbar^2 v_F^2\beta^2}{2a^2}\right)\frac{1}{4}\frac{k_B T}{8\rho_M \hbar^2\left(v_s v_F\right)^2}$$

Deformation potential D^2

S. Ono and K. Sugihara, J. Phys. Soc. Jap. **21**, 861 (1966)
L. Pietronero, S. Strässler, and H. R. Zeller, Phys. Rev. B **22**, 904 (1980)
F. G., J. Phys. C **14**, 3345 (1981)
K. Sugihara, Phys. Rev. B **28**, 2157 (1983)
L. Yang, M. P. Anantram, J. Han, and J. Lu, Phys. Rev. B **60**, 13874 (1999)
M. Verissimo-Alves, R. B. Capaz, B. Koiller, E. Artacho, and H. Chacham, Phys. Rev. Lett. **86**, 3372 (2001)
E. H. Hwang and S. Das Sarma, Phys. Rev. B **77**, 115449 (2008)
J. H. Chen, C. Jang, S. Xiao, M. Ishigami, and M. S. Fuhrer, Nature Nanotechnology **3**, 2006 (2008)
S. D. Sarma, S. Adam, E. H. Hwang, and E. Rossi (2010), arXiv:1003.4731
S.-M. Choi, S.-H. Jhi, and Y.-W. Son, Phys. Rev. B **81**, 081407 (2010)

$$g \approx 4\,eV$$

Deformation

Examples

dislocation

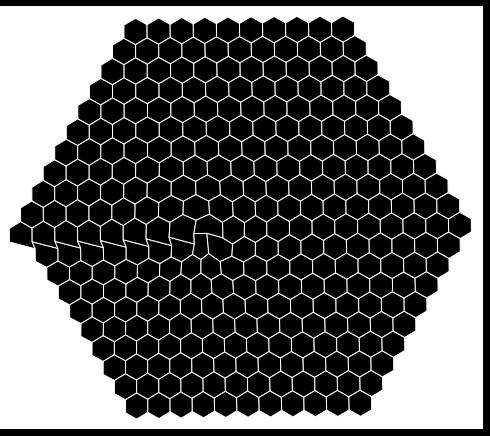

$$u_r = a\,r^3 \sin(4\theta)$$
$$u_\theta = a\,r^3 \cos(4\theta)$$

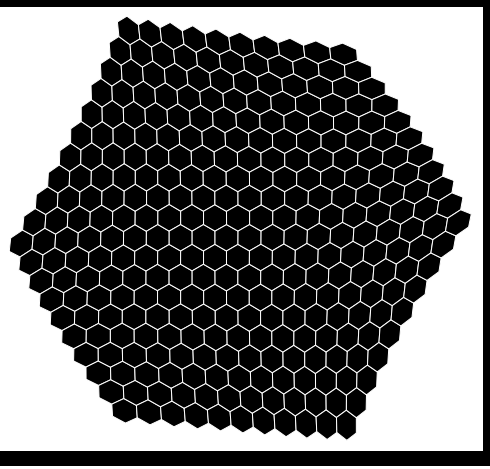

$$u_r = a\,r^4 \sin(5\theta)$$
$$u_\theta = a\,r^4 \cos(5\theta)$$

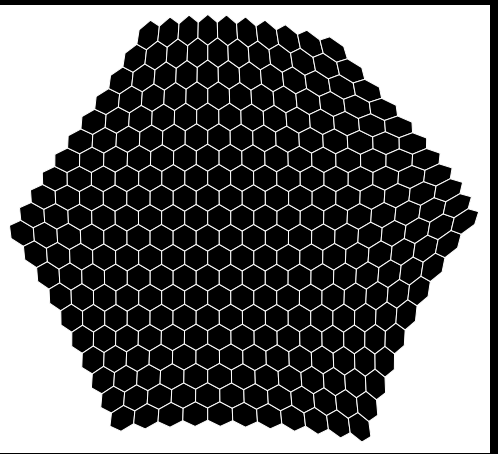

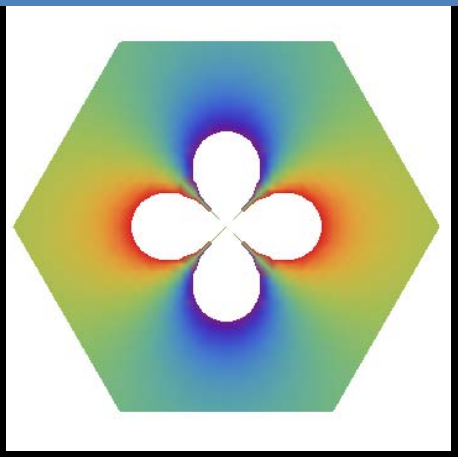

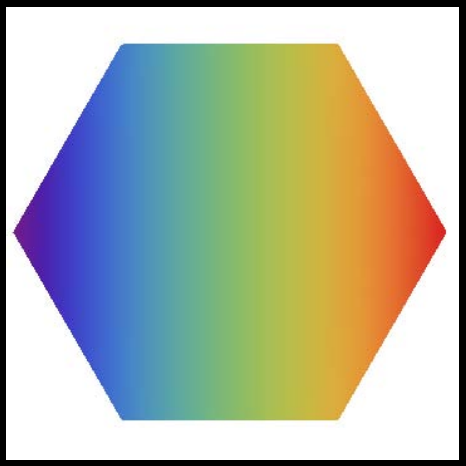

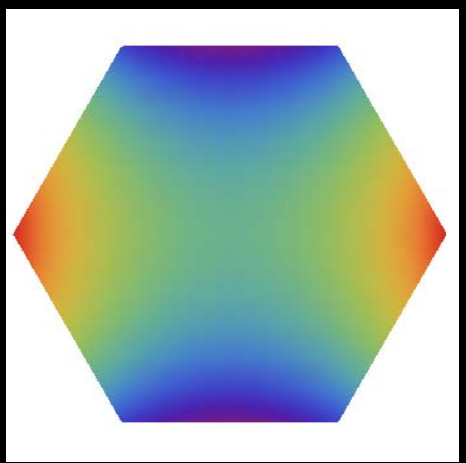

Effective magnetic field

Uniaxial strain

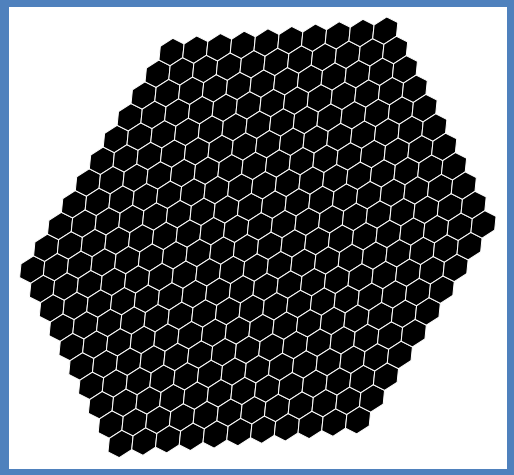

$$u_r = a\,r\sin(2\theta)$$
$$u_\theta = a\,r\cos(2\theta)$$

$$A_y = const$$
$$B = 0$$

M. M. Fogler, F. G., M. I. Katsnelson, Phys. Rev. Lett. **101**, 226804 (2008),

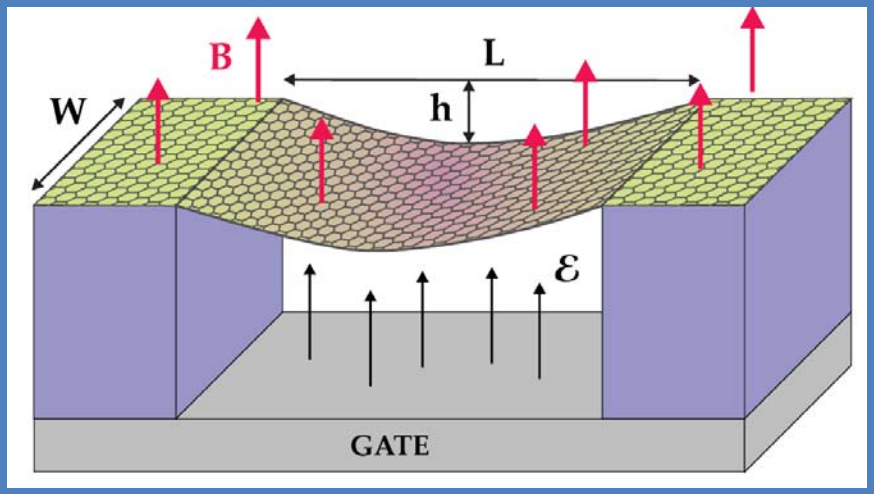

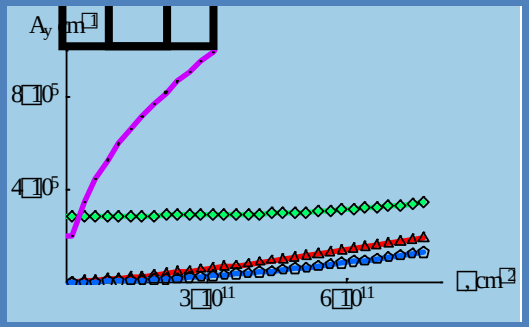

Vector potential inside the suspended region as function of carrier density for different values of the slack

- The graphene layer is deformed by the applied electric field, slack, …
- Stresses lead to effective gauge potentials

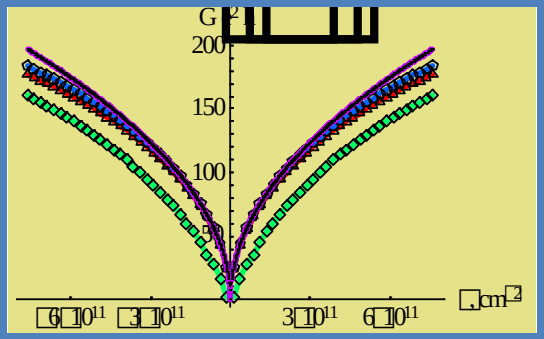

Transmission through a deformed graphene sheet as function of density for different values of the slack

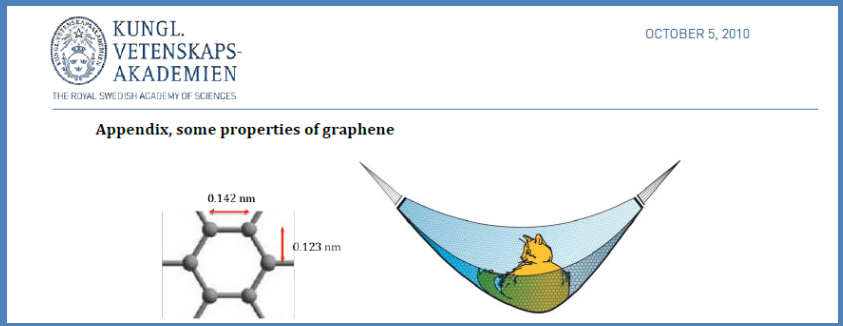

Trigonal distortion (constant effective magnetic field)

F. G., M. I. Katsnelson, A. K. Geim, Nature Phys. **6**, 30 (2010)

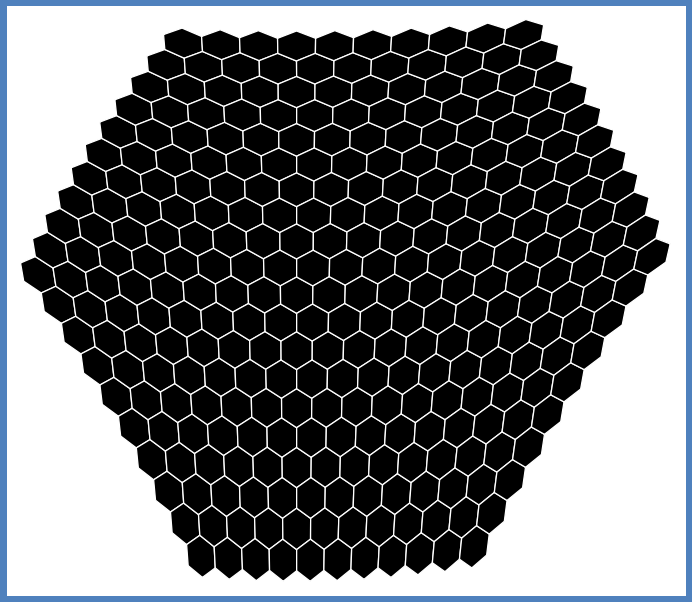

$$u_r = a r^2 \sin(3\theta)$$
$$u_\theta = a r^2 \cos(3\theta)$$
$$u_x = 2axy$$
$$u_y = a(x^2 - y^2)$$

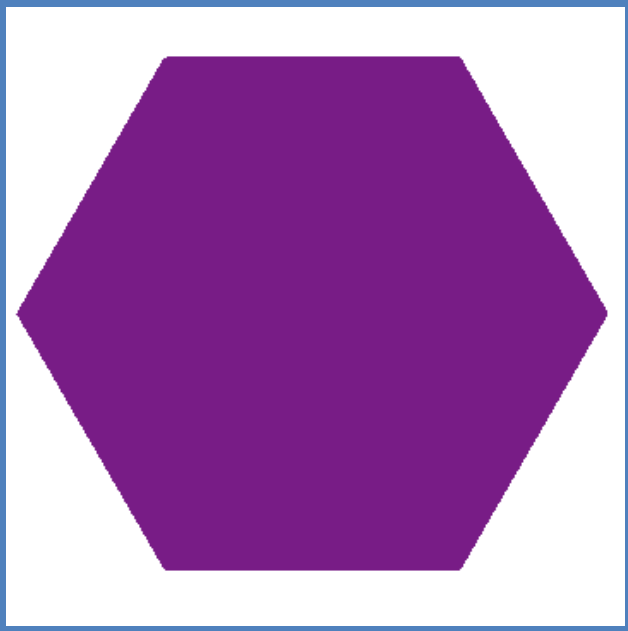

$$u_r = a_r r^m e^{in\theta}$$
$$u_\theta = a_\theta r^m e^{in\theta}$$

n	a_θ/a_r	$B(r,\theta)$
$-m-1$	$-i$	$4im(m-1)e^{-i(m-2)\theta}r^{m-2}$
$-m+1$	$-i\frac{\lambda(m+1)+\mu(m+3)}{\lambda(m-1)+\mu(m-3)}$	$4im(m-1)(m-2)\frac{\lambda+\mu}{\lambda(m-1)+\mu(m-3)}e^{-i(m-4)\theta}r^{m-2}$
$m-1$	$i\frac{\lambda(m+1)+\mu(m+3)}{\lambda(m-1)+\mu(m-3)}$	$-4im(m-1)(m-2)\frac{\lambda+\mu}{\lambda(m-1)+\mu(m-3)}e^{i(m-4)\theta}r^{m-2}$
$m+1$	i	$-4im(m-1)e^{i(m-2)\theta}r^{m-2}$

Strained quantum dot

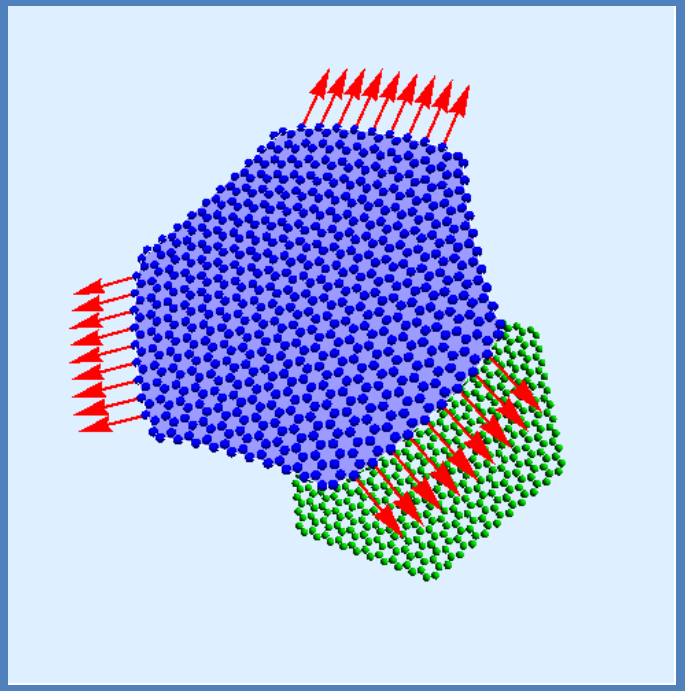

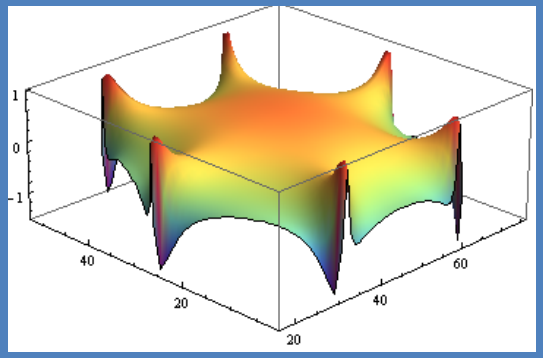

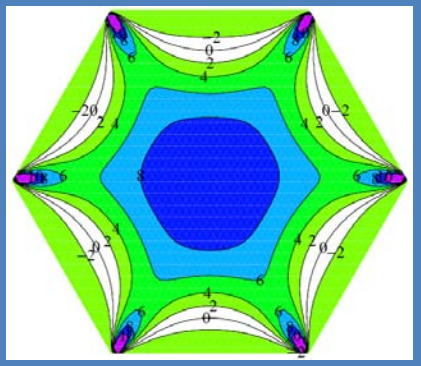

Effective magnetic field

$$\ell_B = \sqrt{\frac{aD}{8\beta\,\Delta_m}}$$

$$D = 100\ nm$$

$$\Delta_m = 10\%$$

$$\ell_B = 4\ nm$$

$$B_{eff} \approx 40T$$

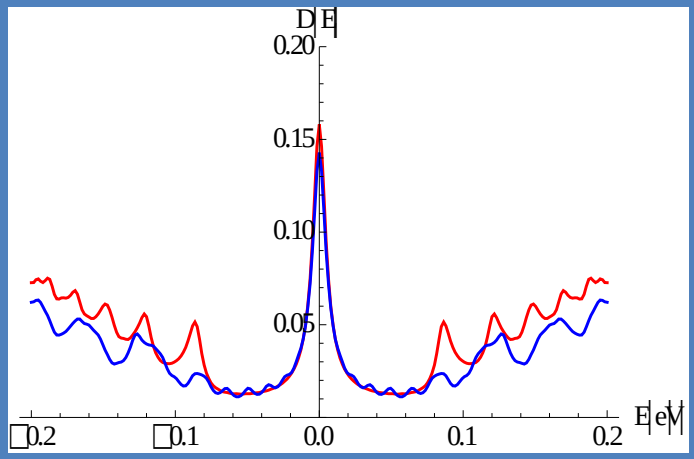

Density of states

Electronic properties

Counterpropagating edge currents

Insulating bulk

Backscattering at the edges

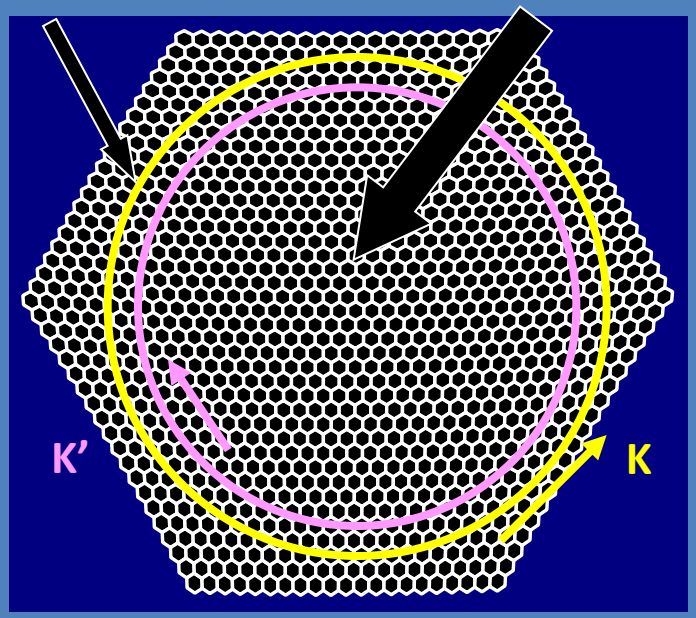

$$\xi \approx \left(\frac{v_F}{e^2}\right)^2 \frac{\ell_B}{n_{imp}^{2D} a^2}$$ charged impurities

$$\xi \approx \frac{\ell_B^2}{n_{def}^{1D} a^2}$$ edge roughness

$$\ell_B \approx 8nm \quad (8T)$$

$$n_{imp}^{2D} \approx 10^{11} cm^{-2} \qquad \xi \approx 10^2 - 10^3 \mu m$$

$$n_{def}^{1D} \approx 10 nm^{-1} \qquad \xi \approx 10^2 - 10^3 nm$$

Two probe transport measurement (Corbino geometry)→oscillating ρ_{xx}

Dissipative edge currents

Other deformations: wrinkles, scrolls, folds, …

Interaction effects can lead to the breaking of time reversal symmetry, turning the material into topological insulator, see I. F. Herbut, Phys. Rev. B **78**, 205433 (2008)

Bubbles and strains in graphene

N. Levy, S. A. Burke, K. L. Meaker, M. Panlasegui, A. Zettl, F. G., A. H. Castro Neto, M. F. Crommie, Science **329**, 544 (2010)

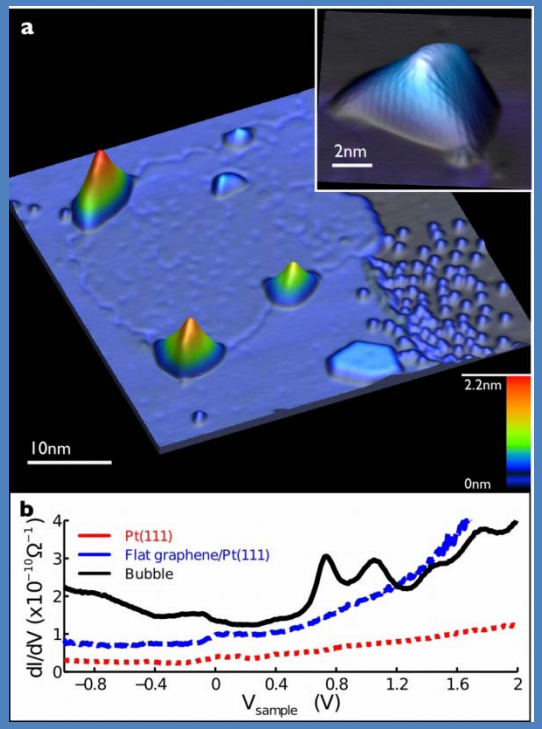

Topography and spectroscopy of bubbles in graphene on Pt

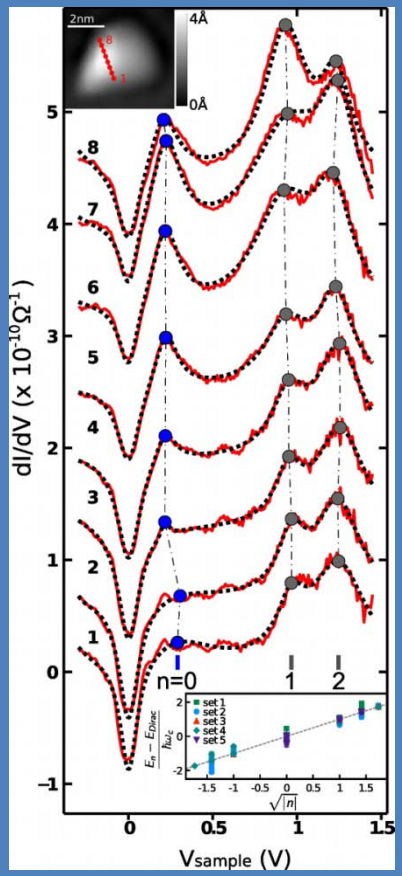

Scaling of resonances observed with STM

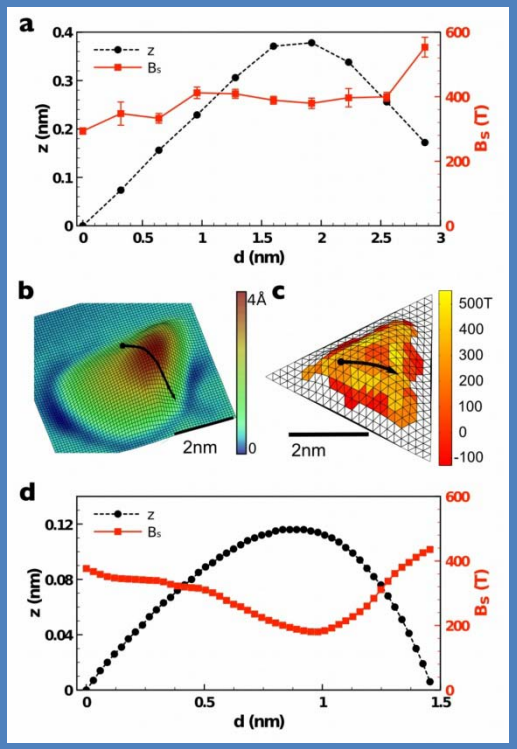

Comparison of theory and experiment

Designer Dirac fermions

LETTER

doi:10.1038/nature10941

Designer Dirac fermions and topological phases in molecular graphene

Kenjiro K. Gomes[1,2*], Warren Mar[2,3*], Wonhee Ko[2,4*], Francisco Guinea[5] & Hari C. Manoharan[1,2]

306 | NATURE | VOL 483 | 15 MARCH 2012

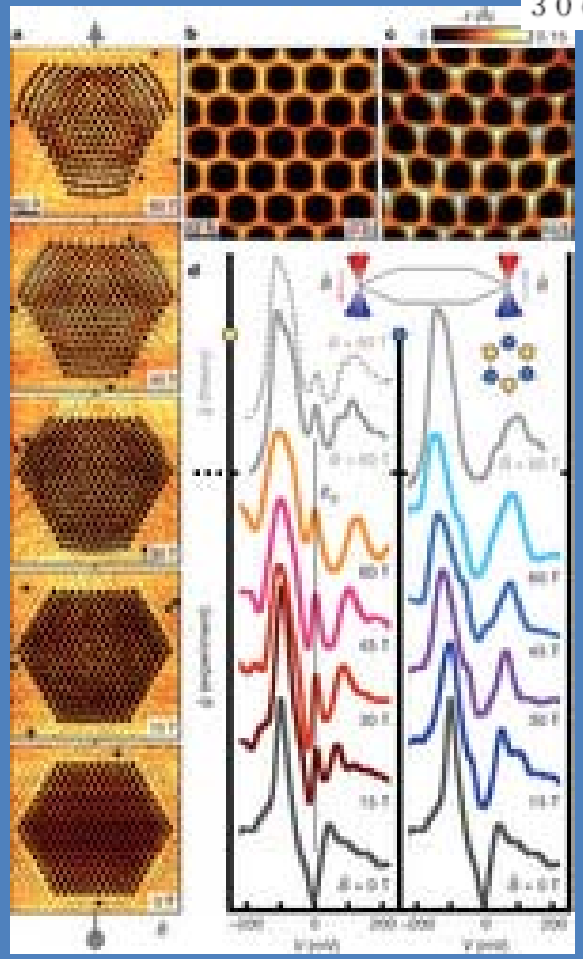

Electromechanical Properties of Graphene Drumheads

Nikolai N. Klimov,[1,2,3] Suyong Jung,[1,2]* Shuze Zhu,[4] Teng Li,[2,4]† C. Alan Wright,[4] Santiago D. Solares,[2,4]† David B. Newell,[3] Nikolai B. Zhitenev,[1] Joseph A. Stroscio[1]†

We determined the electromechanical properties of a suspended graphene layer by scanning tunneling microscopy (STM) and scanning tunneling spectroscopy (STS) measurements, as well as computational simulations of the graphene-membrane mechanics and morphology. A graphene membrane was continuously deformed by controlling the competing interactions with a STM probe tip and the electric field from a back-gate electrode. The probe tip–induced deformation created a localized strain field in the graphene lattice. STS measurements on the deformed suspended graphene display an electronic spectrum completely different from that of graphene supported by a substrate. The spectrum indicates the formation of a spatially confined quantum dot, in agreement with recent predictions of confinement by strain-induced pseudomagnetic fields.

www.sciencemag.org SCIENCE VOL 336 22 JUNE 2012

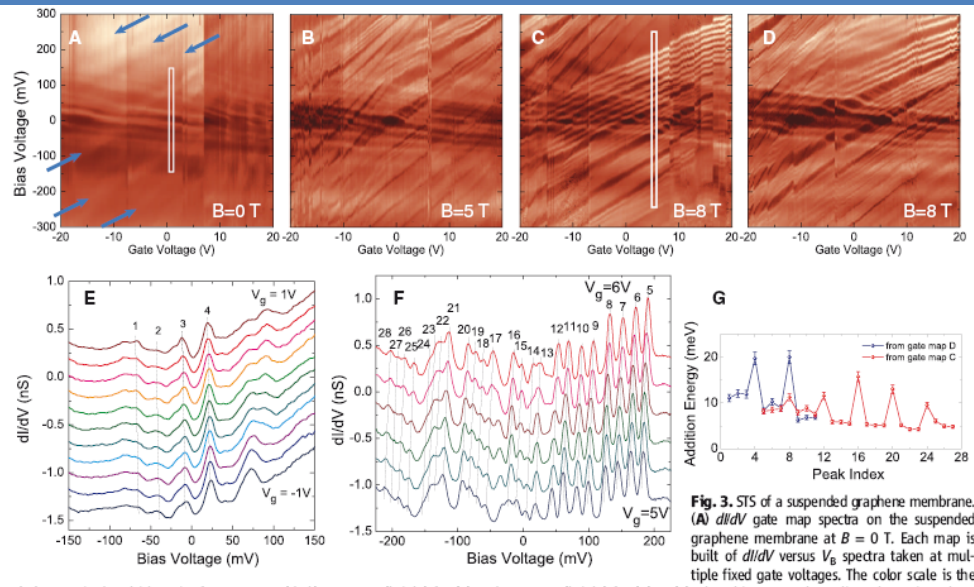

Fig. 3. STS of a suspended graphene membrane. (**A**) *dI*/*dV* gate map spectra on the suspended graphene membrane at $B = 0$ T. Each map is built of *dI*/*dV* versus V_B spectra taken at multiple fixed gate voltages. The color scale is the *dI*/*dV* magnitude, which varies from 0.05 nS (dark) to 1.7 nS (bright) for (A) and to 1.2 nS (bright) for (B) to (D). The white rectangle outlines the region where individual spectra are obtained and plotted in (E). The blue arrows indicate spectral bands with positive slope that become more resolved at higher fields in (B) and (C). (**B** and **C**) *dI*/*dV* gate-map spectra on the suspended graphene membrane at (B) $B = 5$ T and (C) $B = 8$ T. The white rectangle in (C) denotes the region where individual spectra are obtained and plotted in (F). (**D**) *dI*/*dV* gate-map spectra at $B = 8$ T, showing the variability in the measurements when moving off and back on the membrane. (**E**) *dI*/*dV* versus V_B spectra from the $B = 0$ T gate map in (A) for gate voltages varying from −1 to 1 V. (**F**) *dI*/*dV* versus V_B spectra from the $B = 8$ T gate map in (C) for gate voltages varying from 5 to 6 V. The spectra are shifted vertically for clarity in (E) and (F). (**G**) QD addition energies corresponding to the difference in *dI*/*dV* peak positions in the spectra from the gate maps in (C) (red symbols) and (D) (blue symbols). Energies are converted from bias voltages using the lever arm, $E = \alpha V_B$, where $\alpha = 0.45 \pm 0.03$. The error bars in (G) are dominated by the statistical error in α, which was determined from 1-SD uncertainties in the measured slopes of the charging lines in the gate maps. These uncertainties, in turn, determine the corresponding uncertainties in the capacitance ratios discussed in the main text.

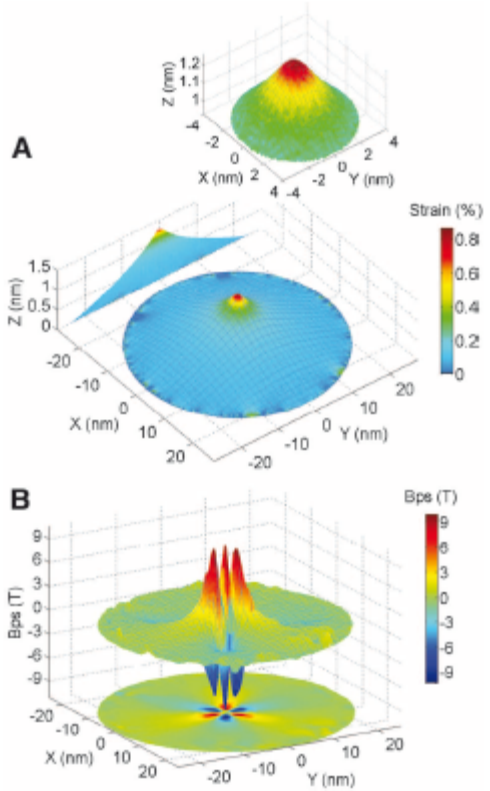

Fig. 4. Simulations of a graphene membrane shape and corresponding strain and pseudomagnetic field. (**A**) Graphene membrane shape with the STM tip positioned over the center of the membrane at zero back gate force. The inset shows a zoomed-in region where the strain is maximal. The radii of the tip and membrane in this model are 2.5 and 25 nm, respectively. (**B**) The pseudomagnetic field, calculated from the strain in (A) (fig. S10) (*18*), shows a spatially alternating field with threefold symmetry that can spatially confine carriers.

Strains and real magnetic fields

Contacts induce strains, which lead to "hot spots"

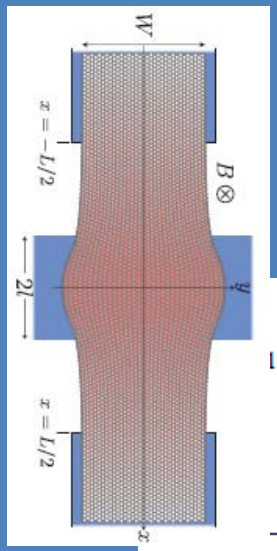

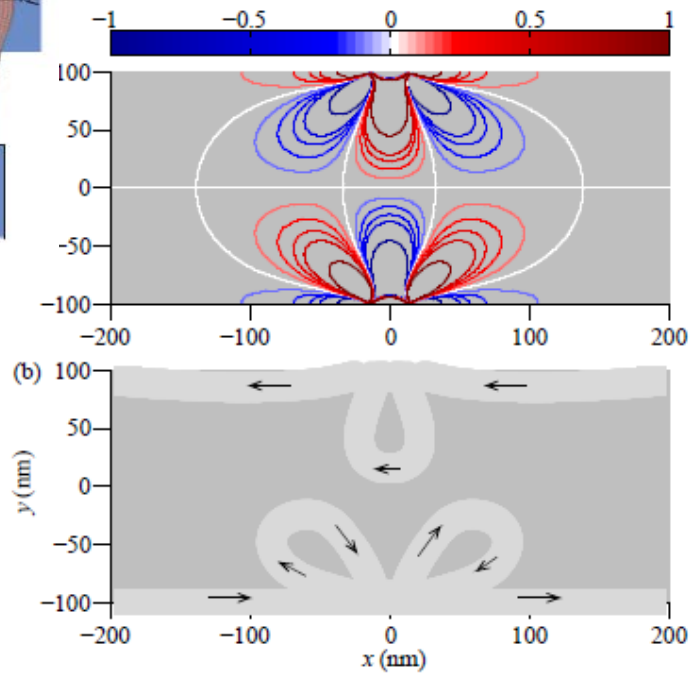

FIG. 3. (Color online). (a) Pseudomagnetic field, in Tesla, induced by two stamps with parameters $2l = 30\,\text{nm}$, $c_0 = 1$ in a sample of width 200 nm. (b) Effect of this pseudomagnetic field on the edge states of the $N = 2$ Landau level at $B = 1\,\text{T}$. The edge states are depicted as light gray ribbons of thickness $\ell \approx 26\,\text{nm}$. The arrows indicate their propagation direction.

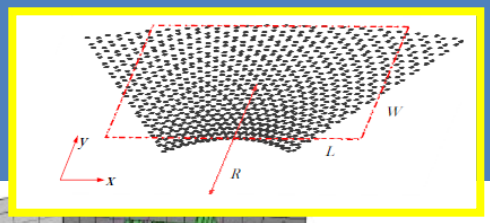

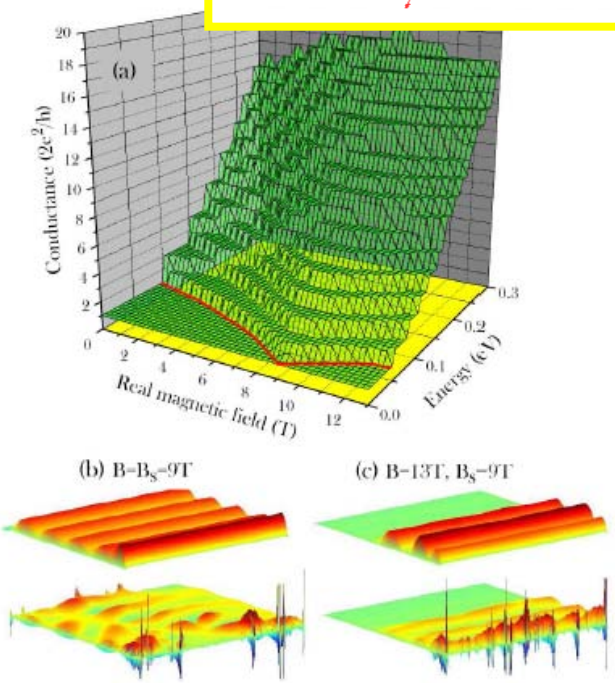

FIG. 6: (a) shows the conductance as a function of real magnetic field and Fermi energy, calculated for non-disordered zigzag ribbon with a strain geometry corresponding to $W/R = 5$, which is equivalent to $B_s \approx 9T$. (b) plots the current density at $\epsilon_f = 0.1eV$ for the condition $B = B_s = 9T$, for perfect edge (top) and disorder edges (bottom). Similar plots for (c), except now for the condition of $B = 13T$ and $B_s = 9T$.

E. Prada, P. San-Jose, G. Leon, M. M. Fogler, F. G., Phys. Rev. B **81**, 161402(R) (2010)

T. Low, F. G. , Nano Lett. **10**, 3551 (2010)

Strains and real magnetic fields

D. Rainis, F. Taddei, M. Polini,, F. Taddei, M. Polini, G. León, F. G., V. I. Fal'ko, Phys. Rev. B **83**, 165403 (2012)
See also E. Prada, P. San José, L. Brey, Phys. Rev. Lett. **105**, 106802 (2010)

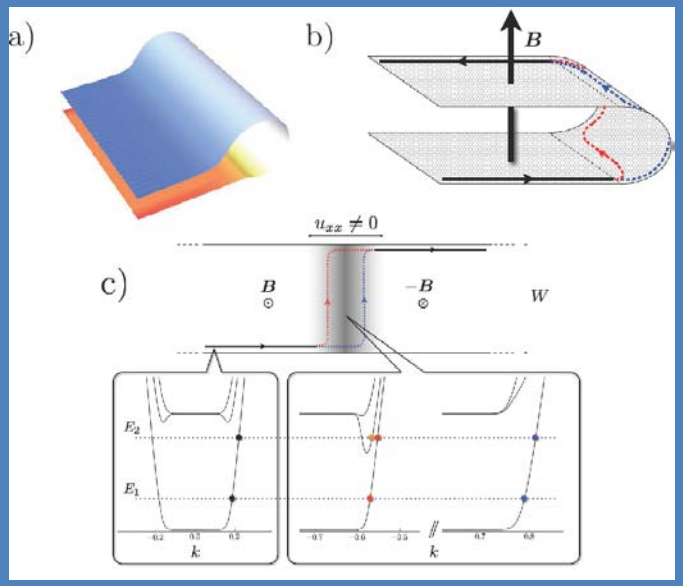

Graphene fold

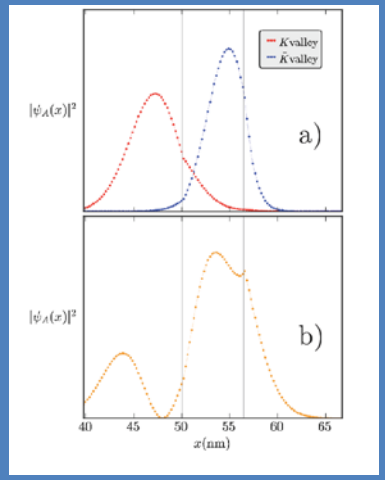

Wave functions of the edge channels

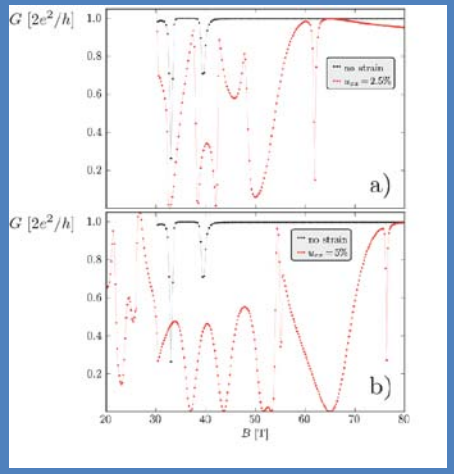

Transmission as function of magnetic field. Fano and Aharonov-Bohm oscillations

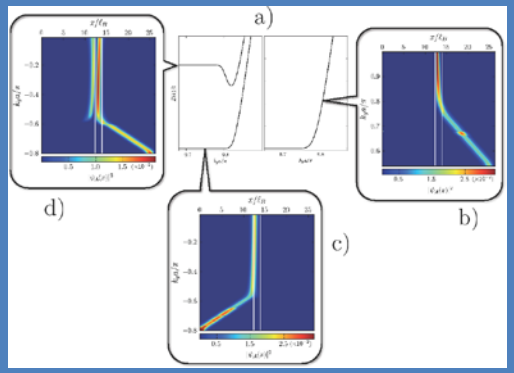

Edge channels

- Edge channels exist at a graphene fold
- Strains split the channels, leading to valley polarization
- The magnetic field between the channels leads to interference patterns

Electron-electron interactions

$$H = H_{kin} + H_{\text{int}} = \hbar v_F \int \overline{\psi} \sigma_i \partial_i \psi + \frac{e^2}{\varepsilon} \int \overline{\psi}(\vec{r}) \psi(\vec{r}) \frac{1}{|\vec{r} - \vec{r}'|} \overline{\psi}(\vec{r}') \psi(\vec{r}')$$

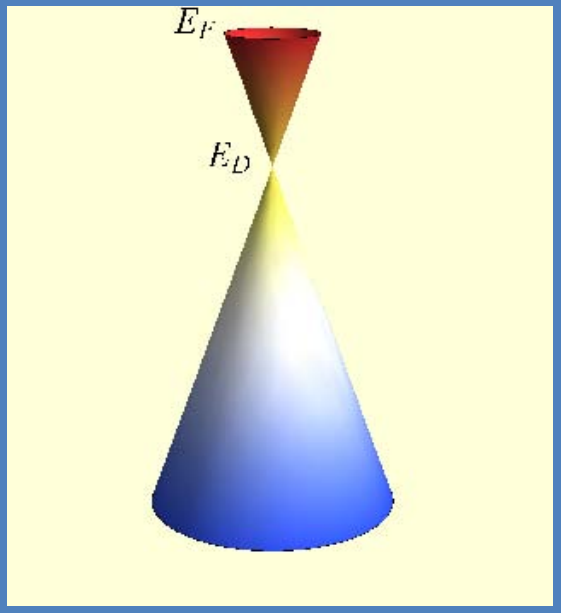

$$E_{kin} \propto \hbar v_F n^{3/2}$$

$$E_{Coulomb} \propto \frac{e^2}{\varepsilon} n^{3/2}$$

$$\alpha = \frac{e^2}{\varepsilon \hbar v_F} \approx 2.3 - 2.5 \quad (\varepsilon = 1)$$

The coupling constant in graphene.

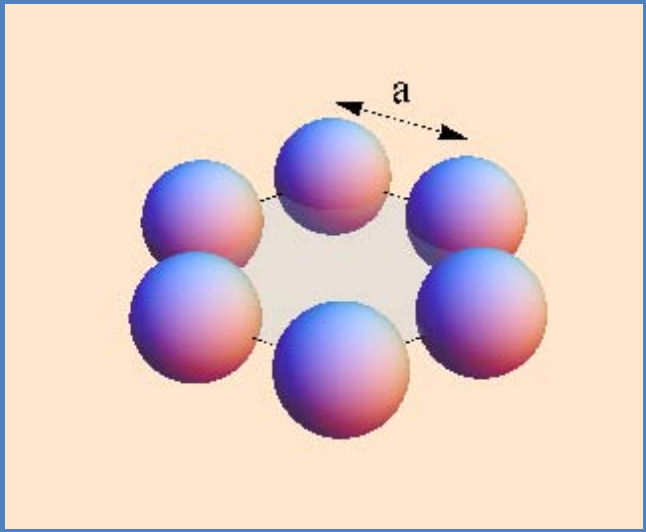

$$E_{kin} = \frac{\hbar^2 k_F^2}{2m} \approx \frac{\hbar^2}{ma^2}$$

$$E_{Coul} \approx -\frac{e^2}{a}$$

The lattice constant of a solid is determined by the balance between the kinetic and potential energies

$$\left.\begin{aligned} E_{kin} = \hbar v_F k_F \Rightarrow \hbar v_F \approx \frac{\hbar^2}{ma} \\ E_{kin} \approx E_{Coul} \Rightarrow \frac{\hbar^2}{ma^2} \approx \frac{e^2}{a} \end{aligned}\right\} \Rightarrow \frac{e^2}{\hbar v_F} \approx 1$$

The “fine estructure constant” in solids is always of order unity.

Screening in graphene

$$\varepsilon_{subs} = \frac{1+\varepsilon_{diel}}{2} \approx \begin{cases} 2.5 & \varepsilon_{SiO_2} \approx 3.9 \\ 5.4 & \varepsilon_{SiC} \approx 9.7 \\ 2.3 & \varepsilon_{BN} \approx 4.5 \end{cases}$$

$$\varepsilon_{graphene}^{RPA} = 1 + \frac{\pi e^2}{2\hbar v_F} \approx 4.6$$

The Effective Fine-Structure Constant of Freestanding Graphene Measured in Graphite

James P. Reed,[1] Bruno Uchoa,[1] Young Il Joe,[1] Yu Gan,[1] Diego Casa,[2] Eduardo Fradkin,[1] Peter Abbamonte[1]*

www.sciencemag.org SCIENCE VOL 330 5 NOVEMBER 2010

(*19*). Extrapolating linearly to zero, we find that $\alpha_g^*(0^+, 0) \equiv \lim_{\mathbf{k}\to 0} \alpha_g^*(\mathbf{k}, 0) = 0.14 \pm 0.092 \approx 1/7$, which may be thought of as a static dielectric constant of $\varepsilon = [1 - Q(\infty)/e]^{-1} = 15.4^{+39.56}_{-6.45}$ (*19*). This large value, which is an outcome of the excitonic shifts shown in Fig. 2B, is 3.5 times as large as past estimates based on the random phase approximation (RPA) (*27*) or GW methods (*26*) in which excitonic effects were neglected. The small value of α_g^* in this limit indicates that graphene can screen very effectively over finite distances and should act like a weakly interacting system for phenomena that take place at low energy and modest wave vector.

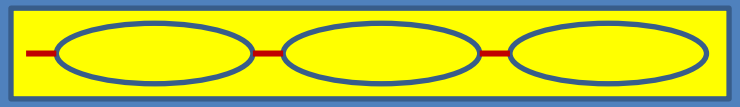

$$\varepsilon_{graphene}^{RPA+vertex} \approx 5.5$$

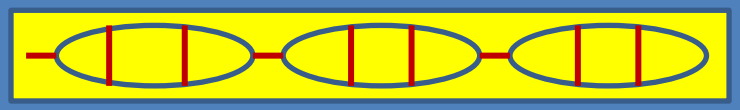

V. N. Kotov, B. Uchoa, A. H. Castro Neto, Phys. Rev. B 80, 165424 (2009)

M. M. Fogler, M. I. Katsnelson, M. Polini, A. Principi, F. G., unpublished

Measurements of α

Observation of Plasmarons in Quasi-Freestanding Doped Graphene

Aaron Bostwick,[1] Florian Speck,[2] Thomas Seyller,[2] Karsten Horn,[3] Marco Polini,[4*] Reza Asgari,[5*] Allan H. MacDonald,[6] Eli Rotenberg[1]†

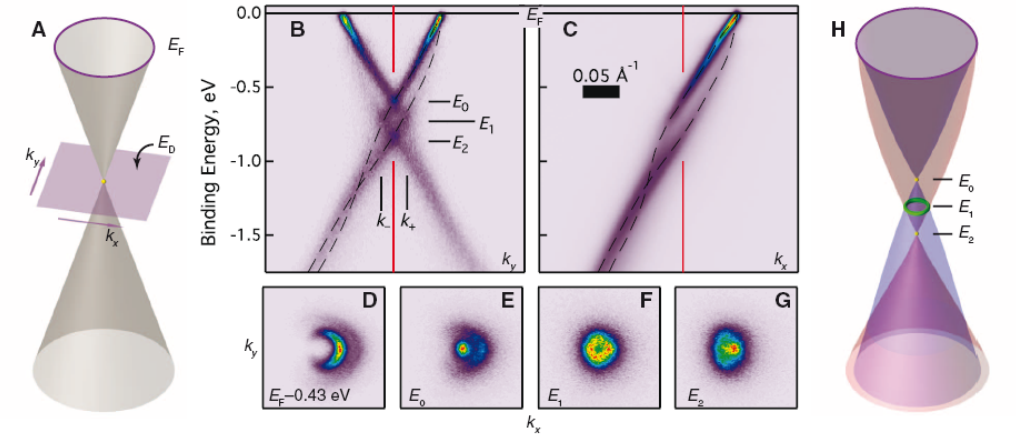

Fig. 1. (**A**) The Dirac energy spectrum of graphene in a non-interacting, single-particle picture. (**B** and **C**) Experimental spectral functions of doped graphene perpendicular and parallel to the ΓK direction of the graphene Brillouin zone. The dashed lines are guides to the dispersion of the observed hole and plasmaron bands. The red lines are at $k = 0$ (the K point of the graphene Brillouin zone). (**D** to **G**) Constant-energy cuts of the spectral function at different binding energies. (**H**) Schematic Dirac spectrum in the presence of interactions, showing a reconstructed Dirac crossing. The samples used for (B) to (G) were doped to $n = 1.7 \times 10^{13}$ cm^{-2}. The scale bar in (C) defines the momentum length scale in (B) to (G).

α_G were extracted (Fig. 3I). Comparing to our measurements, we conclude that the best fit is for $\alpha_G \sim 0.5$. From this value, we determine the average screening $\varepsilon \sim 4.4$, corresponding to substrate screening contribution $\varepsilon_b \sim 7.8$ for graphene on H-SiC in vacuum.

$$\alpha_G \geq 2$$

Renormalization
Marginal Fermi liquid behavior in graphene

The Fermi velocity increases at low energies
Graphene becomes more insulator-like

$$\Sigma_{HF}(k,\omega)=$$

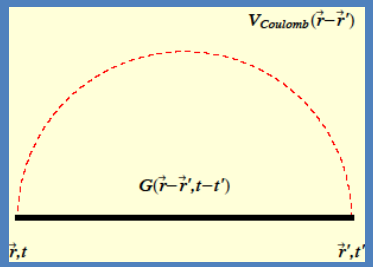

$$\Sigma_{RPA}(k,\omega)=$$

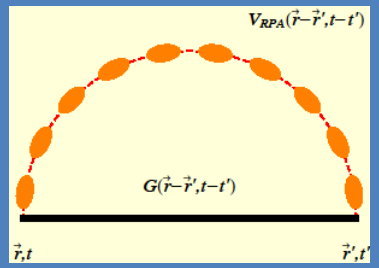

$$\frac{\Lambda}{v_F}\frac{\partial v_F}{\partial \Lambda}=-\frac{e^2}{4\hbar v_F} \qquad \frac{e^2}{\hbar v_F}<<1$$

$$\frac{\Lambda}{v_F}\frac{\partial v_F}{\partial \Lambda}=-\frac{8}{N\pi^2}\left[1-\frac{4\hbar v_F}{Ne^2}+\frac{8\pi v_F\cos^{-1}\left(\frac{\pi Ne^2}{8\hbar v_F}\right)}{\sqrt{1-\left(\frac{\pi Ne^2}{8\hbar v_F}\right)^2}}\right] \qquad \frac{1}{N}<<1$$

$$\mathrm{Im}\,\Sigma\left(\vec{k},\varepsilon_{\vec{k}}\right)=\frac{\pi}{6}\frac{e^2}{\hbar v_F}\left|\varepsilon_{\vec{k}}\right|$$

The lifetime of quasiparticles increases is proportional to the energy

Logarithmic scaling:
A. A. Abrikosov, and D. Benelavski, Soviet, Physics, JETP **32**. 699 (1970).
RG and 1/N expansion: J. González, F. G., M. A. H. Vozmediano, Nucl. Phys. B **424**, 595 (1994), Phys. Rev. B **59**, R2974 (1999),
Quasiparticle lifetime: J. González, F. G., M. A. H. Vozmediano, Phys. Rev. Lett. **77**, 3586 (1996).
See also M. S. Foster, I. L. Aleiner, Phys. Rev. B **77**, 195413 (2008),
V. N. Kotov, B. Uchoa, V. M. Pereira, A. H. Castro Neto, F. G. arXiv:1012.3484, Rev. Mod. Phys., in press.

Excitonic transition?

VOLUME 87, NUMBER 24 PHYSICAL REVIEW LETTERS 10 DECEMBER 2001

Ghost Excitonic Insulator Transition in Layered Graphite

D. V. Khveshchenko

PHYSICAL REVIEW B **81**, 075429 (2010)

Gap generation and semimetal-insulator phase transition in graphene

O. V. Gamayun,* E. V. Gorbar,† and V. P. Gusynin‡

Stoner criterium

$$U \times N(E_F) \geq 1 \Leftrightarrow \frac{e^2}{\varepsilon |k_F|} \times \frac{|k_F|}{v_F} \approx \frac{e^2}{N v_F} \geq 1$$

Selected for a Viewpoint in *Physics*

PHYSICAL REVIEW B **79**, 165425 (2009)

Lattice field theory simulations of graphene

Joaquín E. Drut[1] and Timo A. Lähde[2]

$$\alpha_c = 1.1 \pm 0.06\,?$$

Viewpoint

GrapheneMesoscopics

Physics 2, 30 (2009) DOI: 10.1103/Physics.2.30

Pauling's dreams for graphene

Antonio H. Castro Neto *Department of Physics, Boston University, 590 Commonwealth Ave., Boston, MA 02215*

Published April 20, 2009

Graphene, believed to be a semimetal so far, might actually be an insulator when suspended freely.

RAPID COMMUNICATIONS

PHYSICAL REVIEW B **82**, 121413(R) (2010)

Variational approach to the excitonic phase transition in graphene

J. Sabio,[1,2] F. Sols,[2] and F. Guinea[1]

$$|\Psi_g\rangle \equiv \left(\alpha_k + \beta_k c^+_{e,k} c_{h,k}\right) |\Psi_0\rangle$$

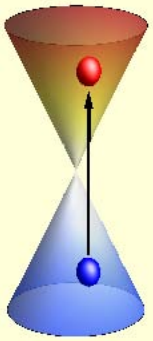

PHYSICAL REVIEW B **82**, 155404 (2010)

Renormalization group approach to chiral symmetry breaking in graphene

J. González

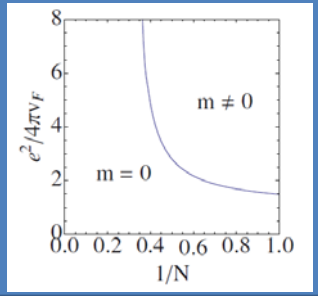

Some early experiments

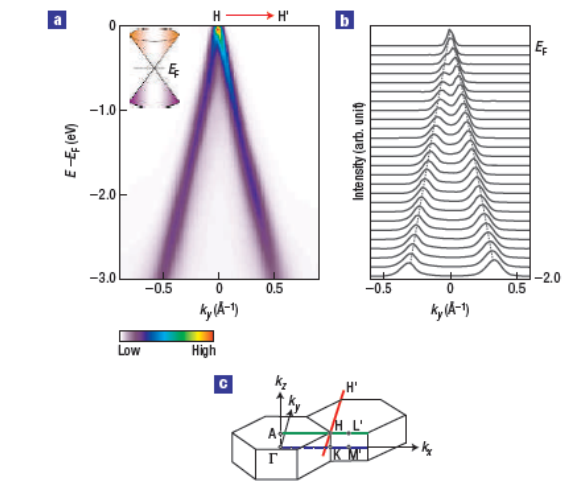

S. Y. Zhou, G.-H. Gweon, J. Graf, A. V. Fedorov, C. D. Spataru, R. D. Diehl, Y. Kopelevich, D.-H. Lee, Steve Louie and A. Lanzara, Nature Phys. **2**, 595 (2006)

The quasiparticle lifetime increases linearly with energy.

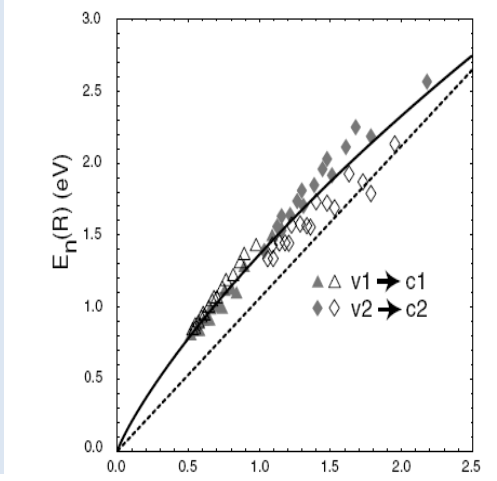

Fabry–Perot interference in a nanotube electron waveguide

Wenjie Liang*†, Marc Bockrath†‡, Dolores Bozovic‡, Jason H. Hafner*, M. Tinkham‡ & Hongkun Park*

$v_F = 8.1 \times 10^5\ \mathrm{m\,s^{-1}}$

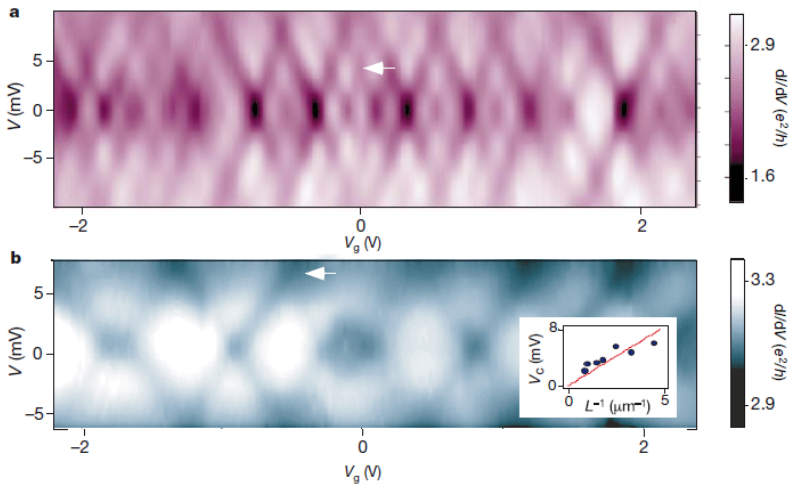

Figure 2 Two-dimensional $\partial I/\partial V$ plots as a function of V and V_g measured at $T = 4$ K. **a**, Data from a 530-nm SWNT device; **b**, data from a 220-nm SWNT device. Both plots show a quasi-periodic pattern of crisscrossing dark lines that correspond to the $\partial I/\partial V$ dips as V and V_g are varied. The bias voltage values (V_c) at which adjacent positively and negatively sloped lines intersect (white arrows) quantify the energy scales for $\partial I/\partial V$ oscillations. In **a**, V_c is ~3.5 meV; in **b**, V_c is ~6.5 meV. Inset, values of V_c from seven devices plotted against the inverse nanotube length (L^{-1}). The solid curve is a line with a slope equal to $hv_F/2 = 1{,}670$ meV nm, where $v_F = 8.1 \times 10^5\ \mathrm{m\,s^{-1}}$ is the Fermi velocity in the nanotube.

Recent experiments

Dirac charge dynamics in graphene by infrared spectroscopy

Z. Q. LI[1]*, E. A. HENRIKSEN[2], Z. JIANG[2,3], Z. HAO[4], M. C. MARTIN[4], P. KIM[2], H. L. STORMER[2,5,6] AND D. N. BASOV[1]

Nature Physics 4, 532 - 535 (2008)
Published online: 8 June 2008 | doi:10.1038/nphys989

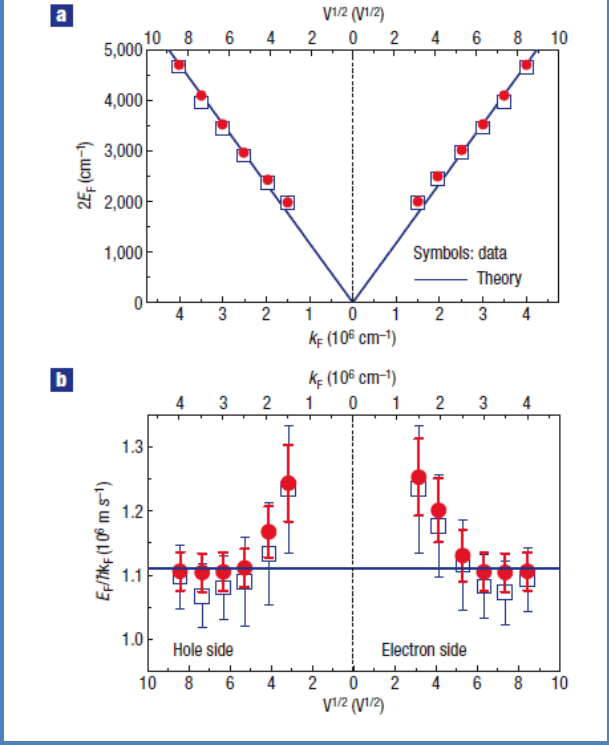

Measurements of the effective mass

Suspended samples. Very high mobility

$\mu \approx 10^6 \mathrm{cm}^2\mathrm{V}^{-1}\mathrm{s}^{-1}$

$n = 1.4\times10^{10}\,\mathrm{cm}^{-2}$

$n = -7\times10^{10}\,\mathrm{cm}^{-2}$

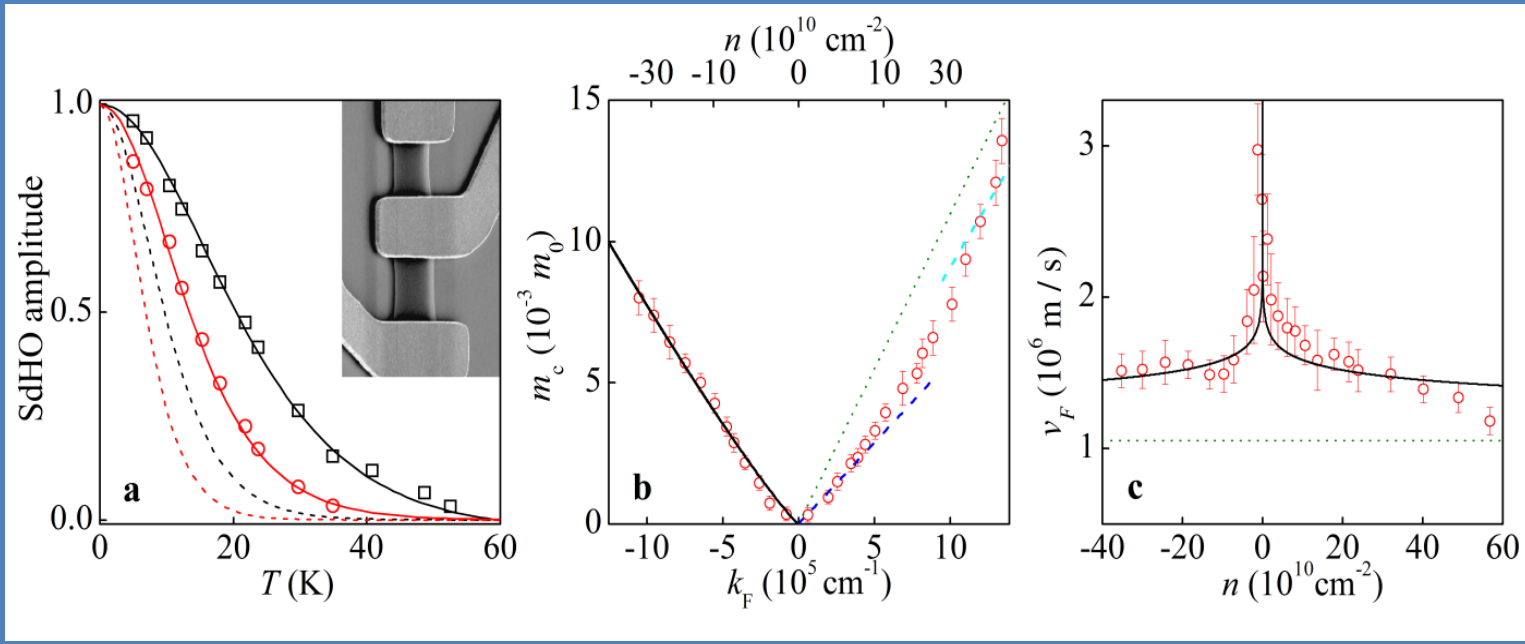

nature physics
LETTERS
PUBLISHED ONLINE: 24 JULY 2011 | DOI: 10.1038/NPHYS2049

Dirac cones reshaped by interaction effects in suspended graphene

D. C. Elias[1], R. V. Gorbachev[1], A. S. Mayorov[1], S. V. Morozov[2], A. A. Zhukov[3], P. Blake[3], L. A. Ponomarenko[1], I. V. Grigorieva[1], K. S. Novoselov[1], F. Guinea[4]* and A. K. Geim[1,3]

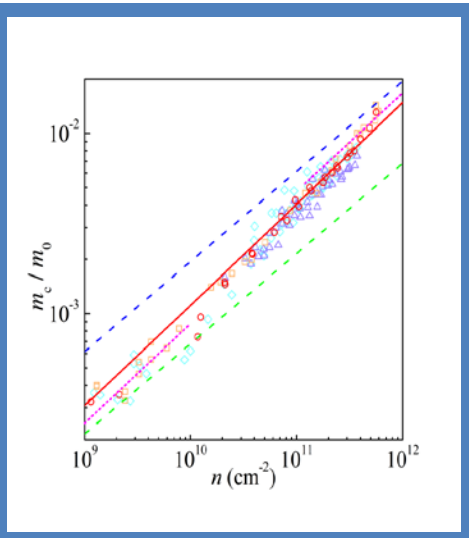

Fits to Renormalization Group calculations

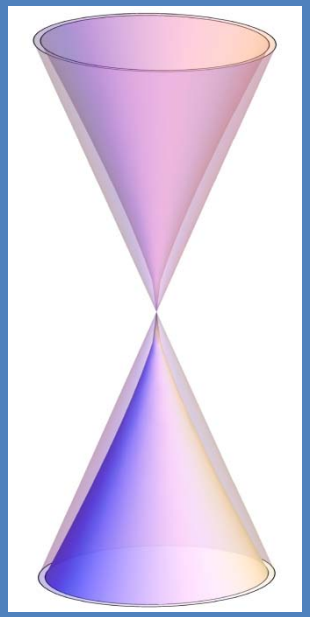

Other recent measurements

PHYSICAL REVIEW B 83, 041405(R) (2011)

Quantized Landau level spectrum and its density dependence in graphene

Adina Luican, Guohong Li, and Eva Y. Andrei

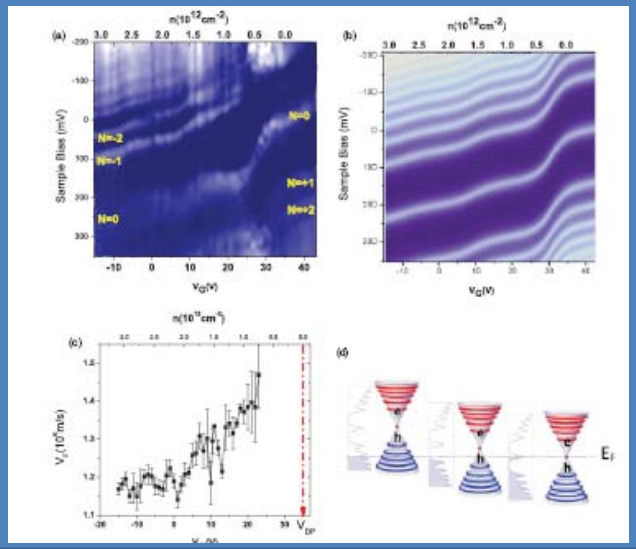

Making ARPES Measurements on Corrugated Monolayer Crystals: Suspended Exfoliated Single-Crystal Graphene

Kevin R. Knox,[1,2] Andrea Locatelli,[3] Mehmet B. Yilmaz,[4] Dean Cvetko,[5,6] Tevfik Onur Mentes,[3] Miguel Ángel Niño,[3,7] Philip Kim,[1] Alberto Morgante,[5,8] and Richard M. Osgood, Jr.[2]

arXiv:1104.2551

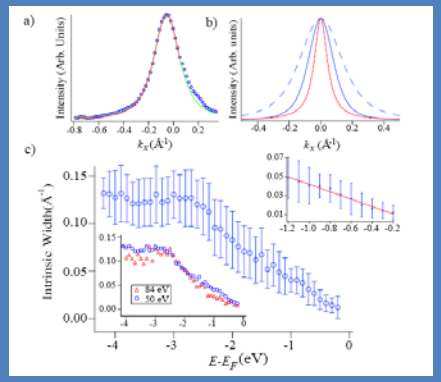

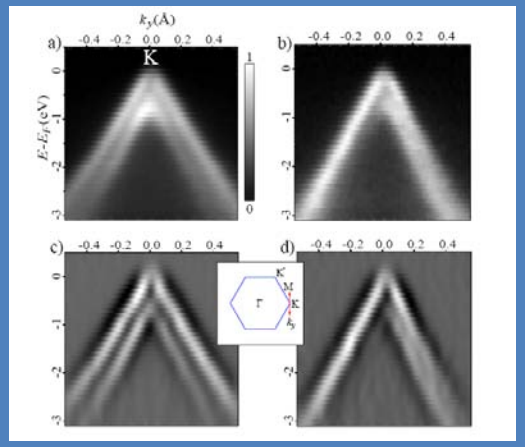

David A. Siegel, Cheol-Hwan Park, Choongyu Hwang, Jack Deslippe, Alexei V. Fedorov, Steven G. Louie, and Alessandra Lanzara, PNAS **108**, 11365 (2011)

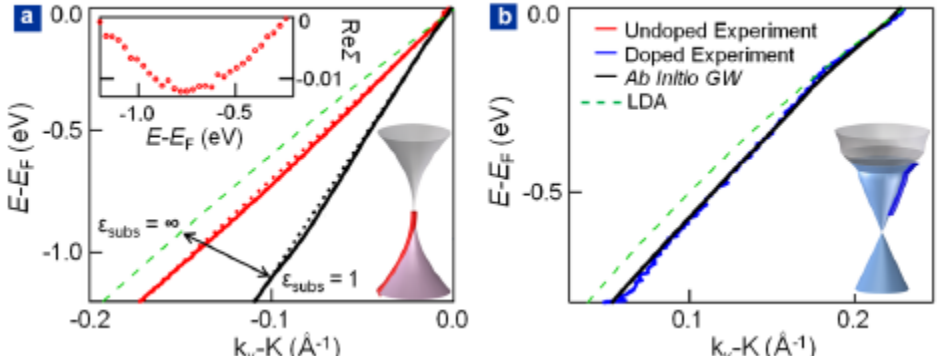

Bilayer graphene

Broken-Symmetry States in Doubly Gated Suspended Bilayer Graphene

R. T. Weitz, M. T. Allen, B. E. Feldman, J. Martin, A. Yacoby*

812 5 NOVEMBER 2010 VOL 330 SCIENCE

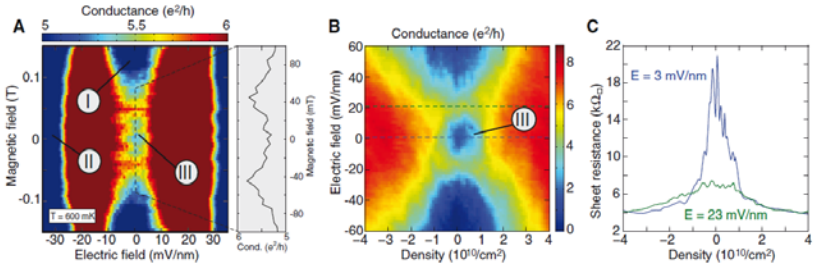

Fig. 4. Experimental evidence of a spontaneous gap in suspended bilayer graphene. **(A)** Detailed view of the conductivity at small electric and magnetic fields and zero average carrier density. The color scale has been restricted to between 5 and 6 e^2/h to highlight the observed effect. **(B)** Conductivity as a function of electric field and density at zero magnetic field. **(C)** Two linecuts showing the resistivity at $E = 0$ and E_{off} are also shown. The scans in (B) and (C) were taken after thermal cycling of the sample, hence the difference in the minimal conductance at zero magnetic and electric field with respect to (A).

PRL 105, 256806 (2010) PHYSICAL REVIEW LETTERS week ending 17 DECEMBER 2010

Local Compressibility Measurements of Correlated States in Suspended Bilayer Graphene

J. Martin, B. E. Feldman, R. T. Weitz, M. T. Allen, and A. Yacoby

VOLUME 61, NUMBER 18 PHYSICAL REVIEW LETTERS 31 OCTOBER 1988

Model for a Quantum Hall Effect without Landau Levels: Condensed-Matter Realization of the "Parity Anomaly"

F. D. M. Haldane

PHYSICAL REVIEW B **77**, 041407(R) (2008)

Pseudospin magnetism in graphene

Hongki Min,[1,*] Giovanni Borghi,[2] Marco Polini,[2] and A. H. MacDonald[1]

PHYSICAL REVIEW B **82**, 115124 (2010)

Quantum anomalous Hall state in bilayer graphene

Rahul Nandkishore and Leonid Levitov

Broken time reversal symmetry.
Ground state similar to the Integer Quantum Hall Effect

PHYSICAL REVIEW B **73**, 214418 (2006)

Electron-electron interactions and the phase diagram of a graphene bilayer

Johan Nilsson,[1] A. H. Castro Neto,[1] N. M. R. Peres,[2] and F. Guinea[3]

Magnetic ground state

PHYSICAL REVIEW B **81**, 041401(R) (2010)

Many-body instability of Coulomb interacting bilayer graphene: Renormalization group approach

Oskar Vafek and Kun Yang

PHYSICAL REVIEW B **82**, 201408(R) (2010)

Spontaneous symmetry breaking and Lifshitz transition in bilayer graphene

Y. Lemonik,[1] I. L. Aleiner,[1,2] C. Toke,[3] and V. I. Fal'ko[2,3]

Nematic ground state

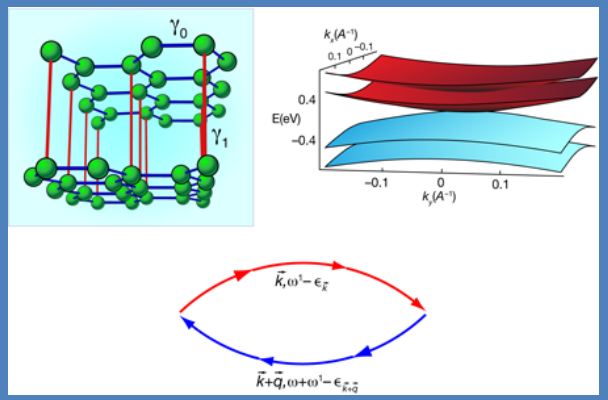

Divergent susceptibilities. Couplings become energy dependent .
F. G., Physics **3**, 1 (2010)

Interaction-Driven Spectrum Reconstruction in Bilayer Graphene

A. S. Mayorov,[1] D. C. Elias,[1] M. Mucha-Kruczynski,[2] R. V. Gorbachev,[3] T. Tudorovskiy,[4] A. Zhukov,[3] S. V. Morozov,[5] M. I. Katsnelson,[4] V. I. Fal'ko,[2] A. K. Geim,[3] K. S. Novoselov[1]*

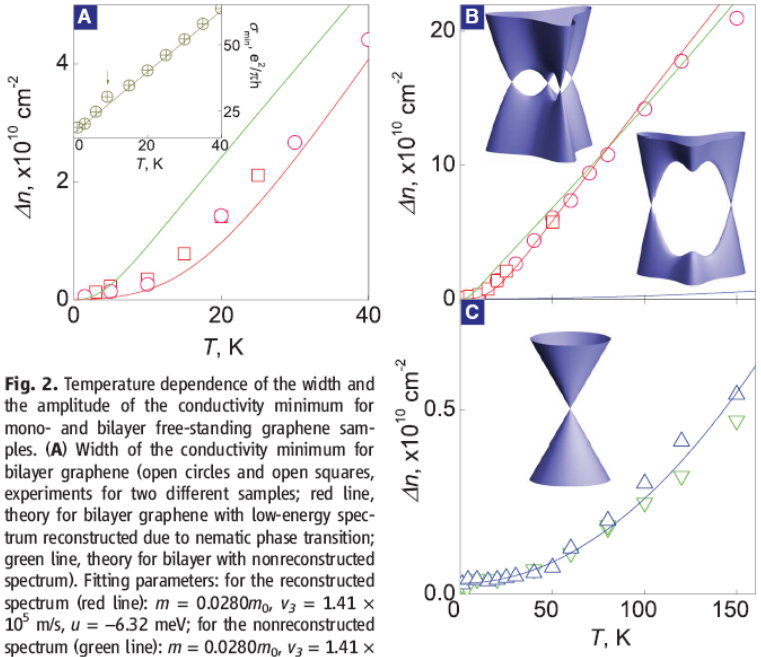

Fig. 2. Temperature dependence of the width and the amplitude of the conductivity minimum for mono- and bilayer free-standing graphene samples. (**A**) Width of the conductivity minimum for bilayer graphene (open circles and open squares, experiments for two different samples; red line, theory for bilayer graphene with low-energy spectrum reconstructed due to nematic phase transition; green line, theory for bilayer with nonreconstructed spectrum). Fitting parameters: for the reconstructed spectrum (red line): $m = 0.0280m_0$, $v_3 = 1.41 \times 10^5$ m/s, $u = -6.32$ meV; for the nonreconstructed spectrum (green line): $m = 0.0280m_0$, $v_3 = 1.41 \times 10^5$ m/s, $u = 0$. (Inset) Amplitude of the conductivity minimum of bilayer graphene (yellow crossed circles, experiment; yellow solid line, a guide to the eye). Note the deviation from the straight line below 10 K (marked by arrow). (**B**) The broadening of the conductivity minimum for bilayer samples [circles, squares, and red and green lines are the same as in (A) and for monolayer graphene (blue line, theory)]. (Insets) Left: Low-energy electronic spectrum as expected in the single-electron approximation; right: bilayer graphene low-energy electronic spectrum, reconstructed due to nematic phase transition. (**C**) The broadening of the conductivity minimum for monolayer graphene [blue and green triangles: experimental points for two different samples; blue line: theory, same as in (B)]. (Inset) Low-energy electronic spectrum for monolayer graphene.

Transport Spectroscopy of Symmetry-Broken Insulating States in Bilayer Graphene

J. Velasco Jr., L. Jing, W. Bao, Y. Lee, P. Kratz, V. Aji, M. Bockrath, C.N. Lau* and C. Varma

Department of Physics and Astronomy, University of California, Riverside, CA 92521

R. Stillwell and D. Smirnov

National High Magnetic Field Laboratory, Tallahassee, FL 32310

Fan Zhang, J. Jung and A.H. MacDonald

Department of Physic, University of Texas at Austin, Austin, TX 78712

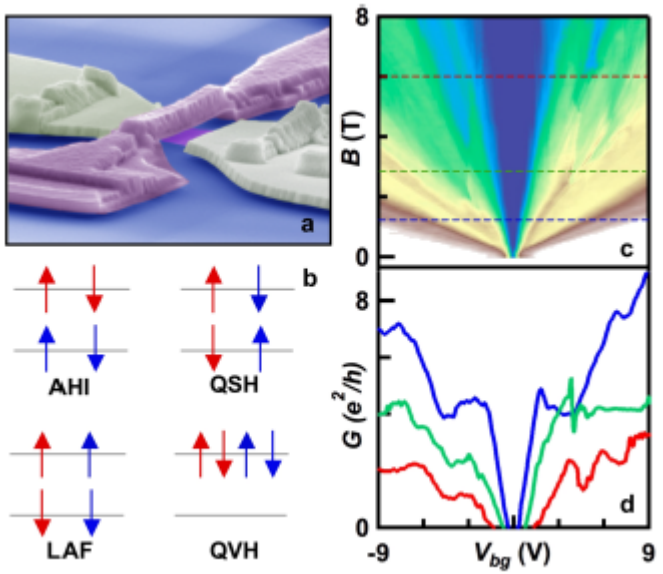

Hybrid structures

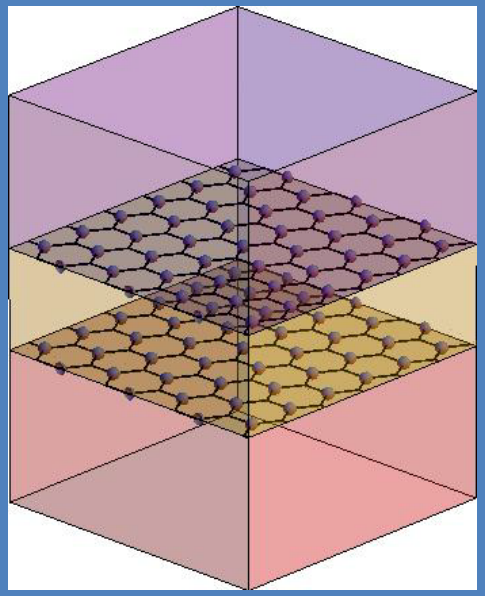

APPLIED PHYSICS LETTERS **99**, 243114 (2011)

Electron tunneling through atomically flat and ultrathin hexagonal boron nitride

Gwan-Hyoung Lee,[1,2] Young-Jun Yu,[3] Changgu Lee,[4] Cory Dean,[1,5] Kenneth L. Shepard,[5] Philip Kim,[3] and James Hone[1,a)]

NANO LETTERS — LETTER — pubs.acs.org/NanoLett

Micrometer-Scale Ballistic Transport in Encapsulated Graphene at Room Temperature

n Britnell,[†] Rashid Jalil,[§] abe,[‖] Takashi Taniguchi,[‖]

Graphene Barristor, a Triode Device with a Gate-Controlled Schottky Barrier

Heejun Yang,[1*] Jinseong Heo,[1*] Seongjun Park,[1] Hyun Jae Song,[1] David H. Seo,[1] Kyung-Eun Byun,[1] Philip Kim,[2] InKyeong Yoo,[1] Hyun-Jong Chung,[1†] Kinam Kim[3]

Science **336**, 1140 (2012); DOI: 10.1126/science.1220527

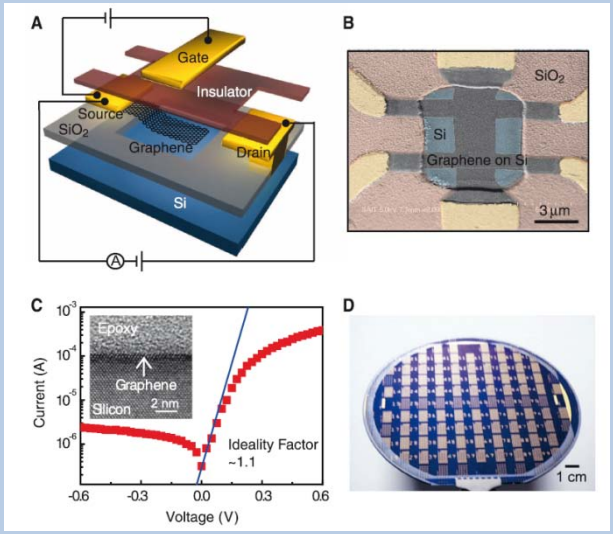

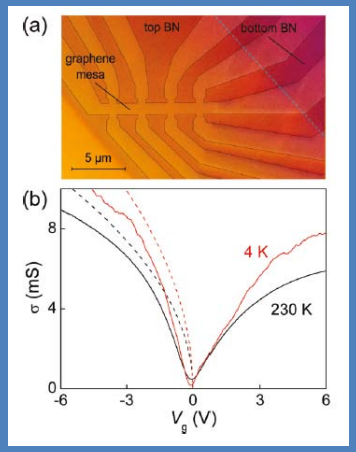

Two graphene layers separated by BN

High carrier mobility

The distance and carrier concentrations can be tuned independently

The graphene layers are electrostatically coupled, screening of puddles, Coulomb drag, …

Superconductivity in graphene

with B. Uchoa, work in progress

Graphite intercalation compounds:

Doped graphene planes.

Superconducting at low temperatures.

T_c=1-11.5K (CaC_6)

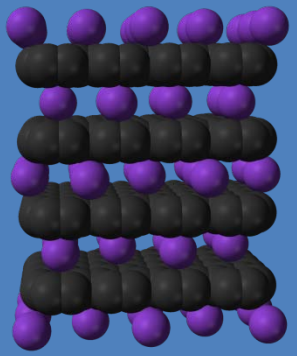

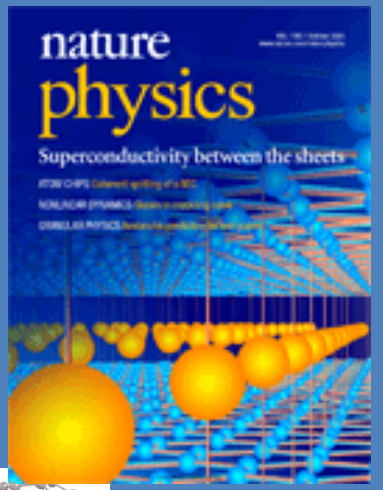

Superconductivity at 18 K in potassium-doped C_{60}

A. F. Hebard, M. J. Rosseinsky, R. C. Haddon, D. W. Murphy, S. H. Glarum, T. T. M. Palstra, A. P. Ramirez & A. R. Kortan

NATURE · VOL 350 · 18 APRIL 1991

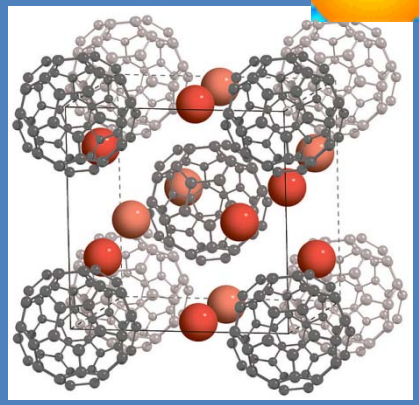

Cs_2RbC_{60} T_c=33K

Phonons?

High carrier density

$n_e/n_C = 1/20 – 1/8$

$n_e = 2\text{-}5 \times 10^{14}\ cm^{-2}$

See also M. Capone, M. Fabrizio, C. Castellani, E. Tosatti, Rev. Mod. Phys. **81**, 943 (2009)

Superconductivity from electron-electron interactions

NEW MECHANISM FOR SUPERCONDUCTIVITY*

W. Kohn

University of California, San Diego, La Jolla, California

and

J. M. Luttinger

Columbia University, New York, New York

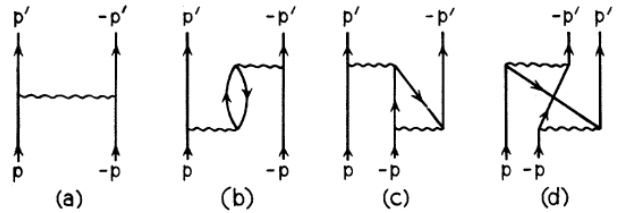

FIG. 1. Types of particle-particle interaction diagrams up to the second order which contribute to the irreducible scattering vertex.

VOLUME 15, NUMBER 12 PHYSICAL REVIEW LETTERS 20 SEPTEMBER 1965

- Metals are always unstable towards superconductivity
- Pairing is mediated by electron-hole pairs
- The natural energy scale is the Fermi energy
- In isotropic three dimensional metals, pairing occurs in a reduced part of the Fermi surface

$$T_{c,n} \approx 1.1 E_F e^{-1/\lambda_n}$$

$$\lambda_n \approx -\frac{2\rho(E_F)}{\pi}\int V\left[2k_F \sin\left(\frac{\theta}{2}\right)\right]\cos(n\theta)d\theta$$

Superconductivity in hybrid structures

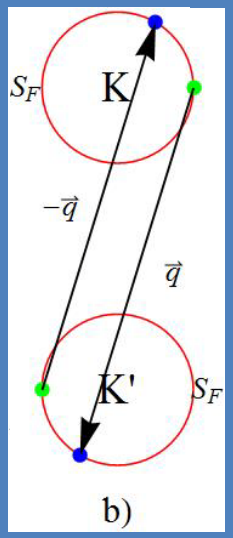

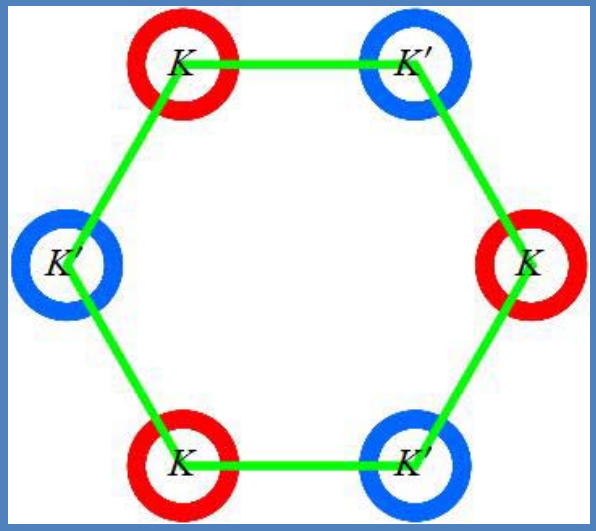

$$T_c \approx E_F e^{-1/\lambda}$$

$$\lambda_{inter} = \frac{\rho(\varepsilon_F)}{\pi}\int_0^{\pi} V\left[2k_F \sin\left(\frac{\theta}{2}\right)\right]\cos^2\left(\frac{\theta}{2}\right)d\theta - \frac{\rho(\varepsilon_F)U\,\Omega}{\pi}$$

- Anisotropic, p-wave superconductivity Finite gap at the Fermi surface
- Short range scattering is pair breaking
- Strong dependence on density

Critical temperature

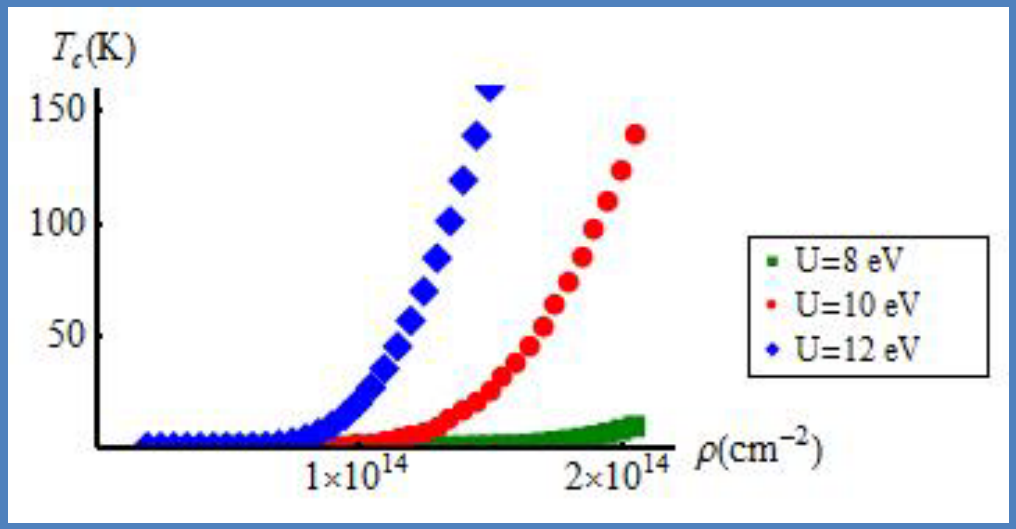

Dependence on U

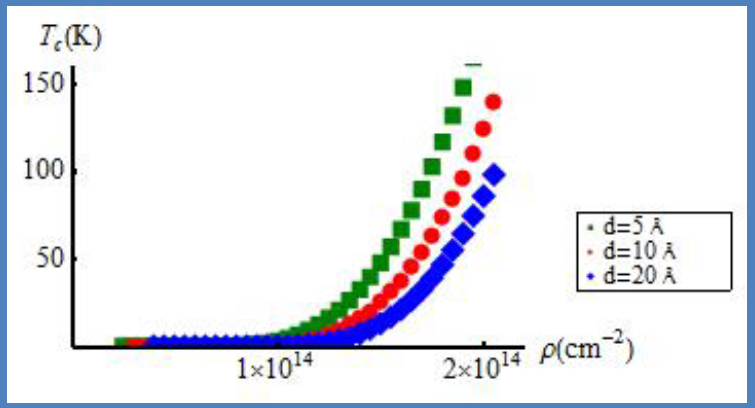

Dependence on d

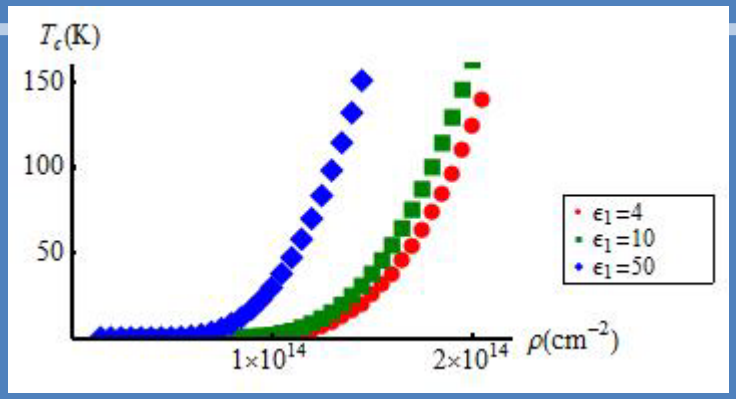

Dependence on ε

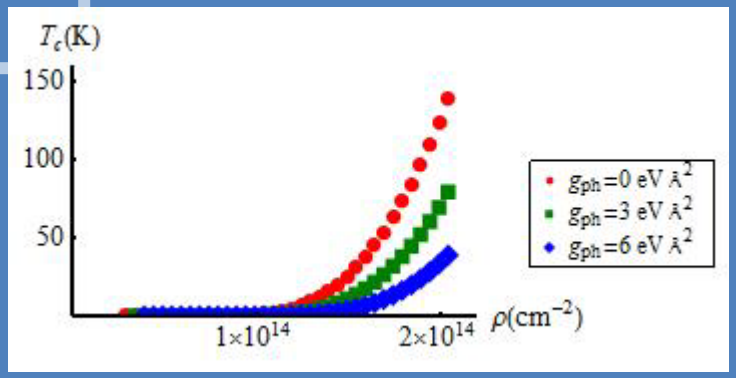

Electron-phonon coupling

Phase fluctuations reduce T_c, see V. M. Loktev, V. Turkowsky, Phys. Rev. B **79**, 233402 (2009)

What next?

- Multilayered graphene.
- Magnetism
- Functionalization
- Optoelectronics, plasmonics, spintronics.
- Novel devices: What can be done with graphene that cannot be done with other materials?
- Can graphene be divided by 4?
- …